


# Visual Mamba: A Survey and New Outlooks

Rui Xu · Shu Yang · Yihui Wang · Yu Cai · Bo Du · Hao Chen 

Received: date / Accepted: date

**Abstract** Mamba, a recent selective structured state space model, excels in long sequence modeling, which is vital in the large model era. Long sequence modeling poses significant challenges, including capturing long-range dependencies within the data and handling the computational demands caused by their extensive length. Mamba addresses these challenges by overcoming the local perception limitations of convolutional neural networks and the quadratic computational complexity of Transformers. Given its advantages over these mainstream foundation architectures, Mamba exhibits great potential to be a visual foundation architecture. Since January 2024, Mamba has been actively applied to diverse computer vision tasks, yielding numerous contributions. To help keep pace with the rapid advancements, this paper reviews visual Mamba approaches, analyzing over 200 papers. This paper begins by delineating the formulation of the orig-

inal Mamba model. Subsequently, it delves into representative backbone networks, and applications categorized using different modalities, including image, video, point cloud, and multi-modal. Particularly, we identify scanning techniques as critical for adapting Mamba to vision tasks, and decouple these scanning techniques to clarify their functionality and enhance their flexibility across various applications. Finally, we discuss the challenges and future directions, providing insights into new outlooks in this fast evolving area. A comprehensive list of visual Mamba models reviewed in this work is available at <https://github.com/Ruixxxx/Awesome-Vision-Mamba-Models>.

**Keywords** Mamba · State Space Model · Computer Vision · Application

## 1 Introduction

Artificial intelligence technologies, especially deep learning, have revolutionized numerous application fields. In the field of computer vision (CV), convolutional neural networks (CNNs) utilize local receptive fields and shared weights to process visual data, capitalizing on inductive biases such as locality and spatial invariance (Krizhevsky et al, 2012; Simonyan and Zisserman, 2015; He et al, 2016). Despite their efficient linear computational complexity with respect to image resolution and proficiency in modeling local patterns, CNNs have restricted receptive fields. This restriction limits their capability to capture larger spatial contexts, which is essential for comprehensively understanding scenes or complex spatial relations in tasks that demand global information. In recent years, Vision Transformers (ViTs) (Dosovitskiy et al, 2021), which utilize a self-attention mechanism (Vaswani et al, 2017) to process sequences

Corresponding author: Hao Chen.

Rui Xu, Shu Yang, Yihui Wang are with the Department of Computer Science and Engineering, The Hong Kong University of Science and Technology, Hong Kong, China. E-mail: rui.xu@whu.edu.cn, {syangcw, ywangrm}@connect.ust.hk.

Yu Cai is with the Department of Electronic and Computer Engineering, The Hong Kong University of Science and Technology, Hong Kong, China. E-mail: yu.cai@connect.ust.hk.

Bo Du is with the School of Computer Science, National Engineering Research Center for Multimedia Software, Institute of Artificial Intelligence and Wuhan Institute of Data Intelligence, Wuhan University, Wuhan, China. E-mail: dubo@whu.edu.cn.

Hao Chen is with the Department of Computer Science and Engineering, the Department of Chemical and Biological Engineering and the Division of Life Science, The Hong Kong University of Science and Technology, Hong Kong, China, and HKUST Shenzhen-Hong Kong Collaborative Innovation Research Institute, Futian, Shenzhen, China. E-mail: jhc@cse.ust.hk.

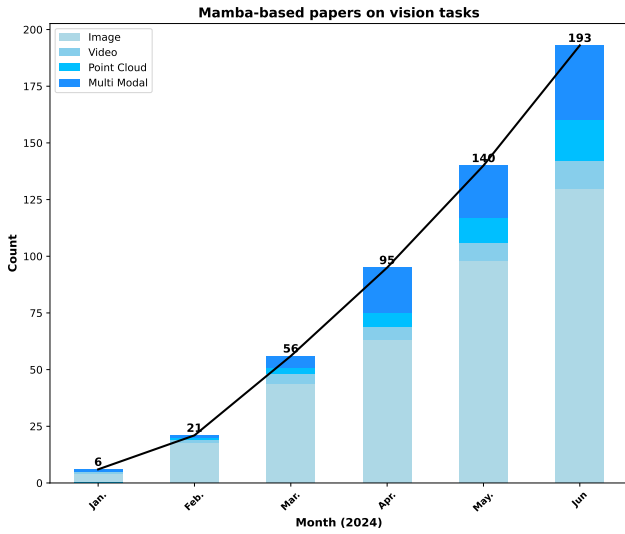


**Fig. 1** The statistics of Mamba-based papers released to date on vision tasks, spanning different modalities including Image, Video, Point Cloud, and Multi-Modal

of image patches, have demonstrated remarkable modeling capabilities across various visual tasks (Liu et al, 2021). Self-attention enables ViTs to capture long-range dependencies within images, providing a significant advantage over traditional CNNs that rely on local receptive fields. This capability allows ViTs to exhibit robust performance on varied datasets and scale effectively to large model sizes. However, the self-attention mechanism involves a quadratic computational cost to the number of patches, which limits the scalability of ViTs. The CV domain has long been dominated by CNNs and ViTs, each with their respective strengths and inherent limitations. To overcome their limitations, researchers have devoted significant effort to improving these models. Recently, structured state space models (Gu et al, 2022b, 2023) have garnered considerable attention due to their computational efficiency and principled capability in modeling long-range dependencies (Gu et al, 2020).

The state space model is a concept that is widely adopted in various disciplines. Its core idea is connecting the input and output sequences using a latent state. It takes different forms in different disciplines, such as Markov decision process in reinforcement learning (Hafner et al, 2020), dynamic causal modeling in computational neuroscience (Friston et al, 2003) and Kalman filters in controls (Kalman, 1960). Recently, the state space model (SSM) has been introduced to deep learning for sequence modeling and its parameters or mappings are learned by gradient descent (Gu et al, 2021). SSM is essentially a type of sequence transformation

and can be incorporated into deep neural networks. It conceptually unifies the strengths of former paradigms for sequence model design, including continuous-time models (CTMs), recurrent neural networks (RNNs), and CNNs. Thereinto, although CNNs are primarily used for processing spatial data and are not sequential, they can be adapted for sequence modeling by leveraging their abilities to encode local contexts and facilitate parallelizable computations. However, SSMs have not been widely used in practice due to their extensive computational and memory requirements coming from the state representation. This situation has changed with the advent of the structured SSM (S4), which addresses these limitations through reparameterizing the state matrices (Gu et al, 2022b). Since then, a series of SSM transformations and neural network architectures incorporating SSM layers emerge (Gu et al, 2022b,a; Gupta et al, 2022; Orvieto et al, 2023; Smith et al, 2023; Gu et al, 2023; Hasani et al, 2023; Fu et al, 2023). However, SSMs' constant sequence transitions restrict their context-based reasoning ability, which is important for the efficacy of models like Transformer (Vaswani et al, 2017). In Mamba (Gu and Dao, 2023), the authors propose to address this by integrating a selection mechanism into the SSM, thus enabling the SSM to selectively propagate or forget information along the sequence or scan path based on the current token. Furthermore, to efficiently compute these selective SSMs, the authors develop a hardware-aware algorithm. Subsequently, the authors integrate these selective SSMs into a simplified neural network architecture, termed Mamba. With the modeling power akin to Transformers and linear scalability in sequence length, Mamba becomes a promising foundation architecture for sequence modeling, which is crucial in the large model era.

Due to the growing adoption of techniques from sequence modeling or natural language processing (NLP) into CV, there is a rapid application of Mamba (Gu and Dao, 2023) to CV tasks (Zhang et al, 2024a; Liu et al, 2024f; Heidari et al, 2024; Zou et al, 2024b). VMamba (Liu et al, 2024g) is an early representative visual Mamba model. It unfolds image patches into sequences along the horizontal and vertical dimensions of the image, and performs bi-directional scanning along these two directions. Another visual Mamba model Vim (Zhu et al, 2024a) leverages position embeddings to incorporate spatial information, inspired by ViT (Dosovitskiy et al, 2021). It also uses bi-directional SSM for handling the non-causal image sequences. Similarly, several other notable studies (Li et al, 2024d; Yang et al, 2024a; Patro and Agneeswaran, 2024b; Huang et al, 2024e; Pei et al, 2024) delve into the exploration of visual backbone networks, consistently achieving compet-

itive performance across classification, detection, and segmentation tasks. To highlight the balance between efficiency and effectiveness in visual Mamba models, Fig. 5 offers a graphical representation contrasting their performance with computational complexity. In addition to these efforts, Mamba has been applied across a diverse range of vision modalities and their respective applications, encompassing image processing, video analysis, point cloud processing, and multi-modal scenarios. Endowed with the aforementioned modeling capability and linear scalability, Mamba stands out as a promising foundation architecture for CV tasks. The growing interest among researchers in applying Mamba to various vision tasks is reflected in the increasing number of studies dedicated to this exploration, as plotted in Fig. 1.

In the rapidly evolving field of CV, Mamba (Gu and Dao, 2023) has emerged as a significant advancement. Keeping pace with the latest research is critical for the community. Therefore, this paper aims to provide a comprehensive review of the applications of Mamba in visual tasks, shedding light on both its foundational elements and diverse applications across various modalities. Our contributions are summarized as follows:

1. **Formulation of Mamba** (Section 2): We provide an introductory overview of the operational principles of the Mamba (Gu and Dao, 2023) and highlight its distinctions from traditional state space models.
2. **Backbone Networks** (Section 3): We provide a detailed examination of several representative visual Mamba backbone networks. This analysis aims to elucidate the core principles and innovations that underpin the visual Mamba framework.
3. **Applications** (Section 4): We categorize applications of Mamba by different modalities, such as image, video, point cloud, and multi-modal data. Each category is explored in depth to highlight how the Mamba framework adapts to and benefits individual modalities.
4. **Challenges and Future Directions** (Section 5): We examine the challenges of visual Mamba models, focusing on their scalability, causality, in-context learning, and trustworthiness. More importantly, we outline prospective directions for visual Mamba models, providing new outlooks into exploring their untapped potential.

## 2 Formulation of Mamba

Mamba (Gu and Dao, 2023) is a recent sequence model aiming at improving the context-based reasoning ability of state space model (SSM) by simply making its

parameters to be functions of the input. The SSM here especially refers to the sequence transformation used in the structured state space sequence model (S4) (Gu et al, 2022b), which can be incorporated into deep neural networks. Mamba simplifies the commonly used SSM block and forms a simplified SSM architecture. In the following, we elaborate on the core concepts of Mamba.

### 2.1 State Space Model

The SSM transformation in S4 (Gu et al, 2022b) originates from the classical state space model, which maps a 1D input signal  $x(t) \in \mathbb{R}$  to a 1D output signal  $y(t) \in \mathbb{R}$  through an N-D latent state  $h(t) \in \mathbb{R}^N$ . This transformation is mathematically formulated as linear ordinary differential equations (ODEs):

$$\begin{aligned} h'(t) &= \mathbf{A}h(t) + \mathbf{B}x(t), \\ y(t) &= \mathbf{C}h(t), \end{aligned} \quad (1)$$

where  $\mathbf{A} \in \mathbb{R}^{N \times N}$  is the evolution parameter and  $\mathbf{B} \in \mathbb{R}^{N \times 1}, \mathbf{C} \in \mathbb{R}^{1 \times N}$  are the projection parameters of neural networks in deep learning. The term  $h'(t)$  denotes the derivative of  $h(t)$  with respect to time  $t$ .

To deal with the discrete input sequence  $\mathbf{x} = (x_0, x_1, \dots) \in \mathbb{R}^L$ , various discretization rules can be used to discretize the parameters in Eq. (1) using a step size  $\Delta$ , which can be seen as the resolution of the continuous input  $x(t)$ . Following previous work (Tustin, 1947), S4 (Gu et al, 2022b) discretizes these parameters using the bilinear method. Following (Gupta et al, 2022), Mamba (Gu and Dao, 2023) employs the zero-order hold (ZOH) assumption<sup>1</sup> to solve the ODEs. Specifically, this results in the conversion of the continuous parameters  $\mathbf{A}, \mathbf{B}$  into their discrete counterparts  $\bar{\mathbf{A}}, \bar{\mathbf{B}}$  as follows:

$$\begin{aligned} \bar{\mathbf{A}} &= \exp(\Delta \mathbf{A}), \\ \bar{\mathbf{B}} &= (\Delta \mathbf{A})^{-1}(\exp(\Delta \mathbf{A}) - \mathbf{I}) \cdot \Delta \mathbf{B}. \end{aligned} \quad (2)$$

After discretizing  $\mathbf{A}, \mathbf{B}$  to  $\bar{\mathbf{A}}, \bar{\mathbf{B}}$ , the Eq. (1) can be reformulated as:

$$\begin{aligned} h_t &= \bar{\mathbf{A}}h_{t-1} + \bar{\mathbf{B}}x_t, \\ y_t &= \mathbf{C}h_t. \end{aligned} \quad (3)$$

Eq. (3) represents a sequence-to-sequence mapping from  $x_t$  to  $y_t$ . This configuration allows the discretized SSM to be computed as RNN. However, due to its sequential nature, this discretized recurrent SSM is impractical for training.

<sup>1</sup> ZOH assumes that the sample value of  $x$  remains constant over each sampling interval  $\Delta$ . For more details on ZOH, refer to [https://en.wikipedia.org/wiki/Zero-order\\_hold](https://en.wikipedia.org/wiki/Zero-order_hold)

For efficient parallelizable training, this recursive process can also be reformulated and computed as a convolution (Gu et al, 2022b):

$$\begin{aligned}\bar{\mathbf{K}} &= (\mathbf{C}\bar{\mathbf{B}}, \mathbf{C}\bar{\mathbf{A}}\bar{\mathbf{B}}, \dots, \mathbf{C}\bar{\mathbf{A}}^{L-1}\bar{\mathbf{B}}), \\ \mathbf{y} &= \mathbf{x} * \bar{\mathbf{K}},\end{aligned}\tag{4}$$

where  $L$  denotes the length of the input sequence  $\mathbf{x}$  and  $*$  represents the convolution operation. The vector  $\bar{\mathbf{K}} \in \mathbb{R}^L$  is the SSM convolution kernel, enabling the simultaneous synthesis of outputs across the sequence. Given  $\bar{\mathbf{K}}$ , the convolution operation in Eq. (4) can be efficiently computed using the fast Fourier transforms (FFTs).

## 2.2 Selective SSM

As seen, the parameters in SSM indicated by either Eq. (1), Eq. (3) or Eq. (4) remain invariant with respect to the input or temporal dynamics. Mamba (Gu and Dao, 2023) identifies this linear time-invariant (LTI) property as a fundamental limitation of SSM when it comes to context-based reasoning. To address this issue, Mamba incorporates a selection mechanism. The selection mechanism is implemented by simply configuring the parameters of SSM as functions of the input, thus achieving input-dependent interactions along the sequence. Specifically, parameters  $\mathbf{B}, \mathbf{C}, \Delta$  are dependent on the input sequence  $\mathbf{x}$ :

$$\begin{aligned}\mathbf{B} &= s_B(\mathbf{x}), \\ \mathbf{C} &= s_C(\mathbf{x}), \\ \Delta &= \tau_\Delta(\text{Parameter} + s_\Delta(\mathbf{x})).\end{aligned}\tag{5}$$

where  $s_B(\mathbf{x}) = \text{Linear}_N(\mathbf{x})$  and  $s_C(\mathbf{x}) = \text{Linear}_N(\mathbf{x})$  both project the input into a dimension  $N$ .  $s_\Delta(\mathbf{x}) = \text{Broadcast}_D(\text{Linear}_1(\mathbf{x}))$  first projects the input to dimension 1, and then broadcasts it to dimension  $D$ .  $\tau_\Delta$  is the *softplus* function. Here we present the complete shape of  $\mathbf{x} \in \mathbb{R}^{B \times L \times D}$ , where  $B$  denotes the batch size,  $L$  is the sequence length, and  $D$  is the number of channels. Accordingly, the parameters  $\mathbf{B}$  and  $\mathbf{C}$  are each shaped as  $\mathbb{R}^{B \times L \times N}$ , and  $\Delta$  is shaped as  $\mathbb{R}^{B \times L \times D}$ .

The resulting selective SSM cannot be computed as either RNN or convolution. Mamba (Gu and Dao, 2023) employs a hardware-aware algorithm to efficiently compute the selective SSM. The hardware-aware algorithm leverages three classical techniques: parallel scan, kernel fusion, and recomputation.

## 2.3 Mamba

Mamba is a simplified SSM architecture, drawing insights from the H3 architecture (Fu et al, 2023), which serves as the basis of many SSM architectures. Specifically, the H3 (Fu et al, 2023) block integrates two discrete SSMs to explicitly simulate linear attention. The commonly used SSM architectures alternately stack the H3 block (Fu et al, 2023) and the MLP block prevalent in modern neural networks. Unlike them, Mamba integrates these two blocks to construct the simplified Mamba block. As illustrated in Fig. 2, the Mamba block can be viewed from two distinct perspectives. Firstly, it replaces the first multiplicative gate in the linear attention-like or H3 (Fu et al, 2023) block with an activation function. Secondly, it incorporates the SSM transformation into the primary pathway of the MLP block. The overall architecture of Mamba consists of repeated Mamba blocks interleaved with standard normalization layers and residual connections.

Mamba inherits the linear scalability in sequence length of the state space models, and also realizes the modeling ability of Transformers. Mamba exhibits the significant advantages of two primary types of foundation architectures in CV, i.e. CNNs and Transformers, making it a promising foundation architecture for CV. In contrast to Transformers, which rely on explicitly storing the entire context for context-based reasoning, Mamba utilizes a selection mechanism, which selectively propagates or filters information along the sequence based on the current token. This ensures the modeling process is influenced solely by the past and current inputs along the sequence, thereby adhering to the principles of causality. Therefore, the 1D and causal characteristics of this selection mechanism become focal points for researchers applying Mamba to CV.

## 3 Visual Mamba Backbone Networks

In this section, we review representative visual Mamba backbone networks to clarify the fundamental principles and innovations of applying Mamba to CV. These backbone networks can be categorized into pure Mamba and hybrid Mamba networks. Pure Mamba networks solely rely on the Mamba architecture for processing visual data, whereas hybrid Mamba networks combine the Mamba architecture with other neural network architectures, such as CNNs and attentions, to capitalize on their complementary advantages.

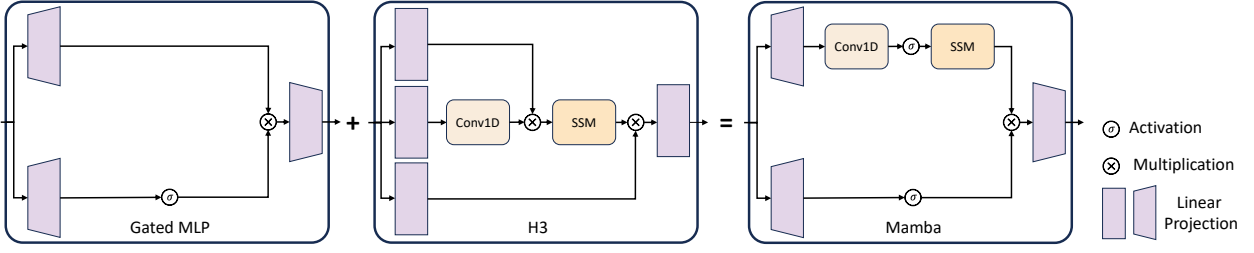


**Fig. 2** Mamba block: a simplified block that integrates the H3 and MLP blocks

### 3.1 Pure Mamba

*Vim*: Vim (Zhu et al, 2024a) is a Mamba-based architecture directly operating on image patch sequences similar to ViT (Dosovitskiy et al, 2021). The input image is first transformed into flattened 2D patches, which are then vectorized using a linear projection layer and added with position embeddings to retain spatial information. Following ViT (Dosovitskiy et al, 2021) and BERT (Devlin et al, 2019), a class token is appended to the sequences of patch tokens. The overall token sequence is then fed into the Vim encoder, which is structured as a series of identical Vim blocks. As illustrated in Fig. 3, the Vim block is a Mamba block integrating a backward SSM path alongside the forward one.

*VMamba*: VMamba (Liu et al, 2024g) identifies the direction-sensitive challenge when applying Mamba to 2D images, due to the 1D causal attribute of its selection mechanism. The selection mechanism makes Mamba unable to assimilate information from the portion of the unscanned data. Therefore, 1D scanning is not optimal for simultaneously capturing the dependency information across different directions of images, leading to restricted receptive fields.

To address the challenge, VMamba introduces a Cross-Scan Module (CSM). The CSM transforms the input image into sequences of patches along both horizontal and vertical axes (*cross-scan*), to scan the sequences in four directions: from the top-left to the bottom-right, the bottom-right to the top-left, the top-right to the bottom-left, and the bottom-left to the top-right. Then the resulting four sequences are individually processed using selective SSMs. This operation can also be seen as performing bi-directional selective SSMs along 2D axes. Consequently, each pixel integrates information from all other pixels in four different directions. Finally, all sequences are transformed into their original 2D layout to constitute maps and merged to obtain the output map (*cross-merge*). The whole process of *cross-scan*, selective SSM, and *cross-merge* constitutes the 2D-Selective-Scan (SS2D).

VMamba first transforms the input image into 2D patches. Then they are fed into multiple stages of VMamba, which are comprised of stacked Visual State Space (VSS) blocks, and down-sampling operations (Liu et al, 2022a) are inserted between these stages to construct the overall hierarchical architecture. VMamba introduces two kinds of VSS blocks, the vanilla VSS block as shown in Fig. 3 and VSS block. The vanilla VSS block is similar to the Mamba block but replaces the 1D convolution layer with a 2D depth-wise convolution layer and the selective SSM with SS2D plus a layer normalization (LN) layer. The VSS block resembles the typical Transformer blocks.

*PlainMamba*: PlainMamba (Yang et al, 2024a) is crafted as a non-hierarchical architecture to fulfill several objectives: (1) a non-hierarchical structure facilitates multi-level feature fusion, enhancing integration across different scales; (2) it supports effective fusion of multi-modal data; (3) its simpler architecture tends to offer better generalization capabilities; (4) it is amenable to optimization for hardware acceleration.

Initially, the input image is transformed into 2D patch tokens, and combined with position embeddings to preserve spatial information. Unlike ViT (Dosovitskiy et al, 2021), no special token, such as the class token, is used. Then these tokens are processed by a series of identical PlainMamba blocks, as shown in Fig. 3. The PlainMamba block is similar to the Mamba block, except that the 2D depth-wise convolution layer is employed to substitute the 1D convolution layer, and more importantly, the selective scanning mechanism of Mamba is adjusted for adapting the 1D operation to 2D images. Firstly, as zigzag scan depicted in Fig. 4, a continuous 2D scanning technique is utilized to ensure the spatial adjacency of tokens and prevent discontinuity. Secondly, a direction-aware updating technique is proposed to explicitly incorporate relative 2D position information into the selective scanning process.

Due to the lack of predefined ordering in visual data and their inherent spatial dimensions, several pure Mamba networks focus on scanning techniques.

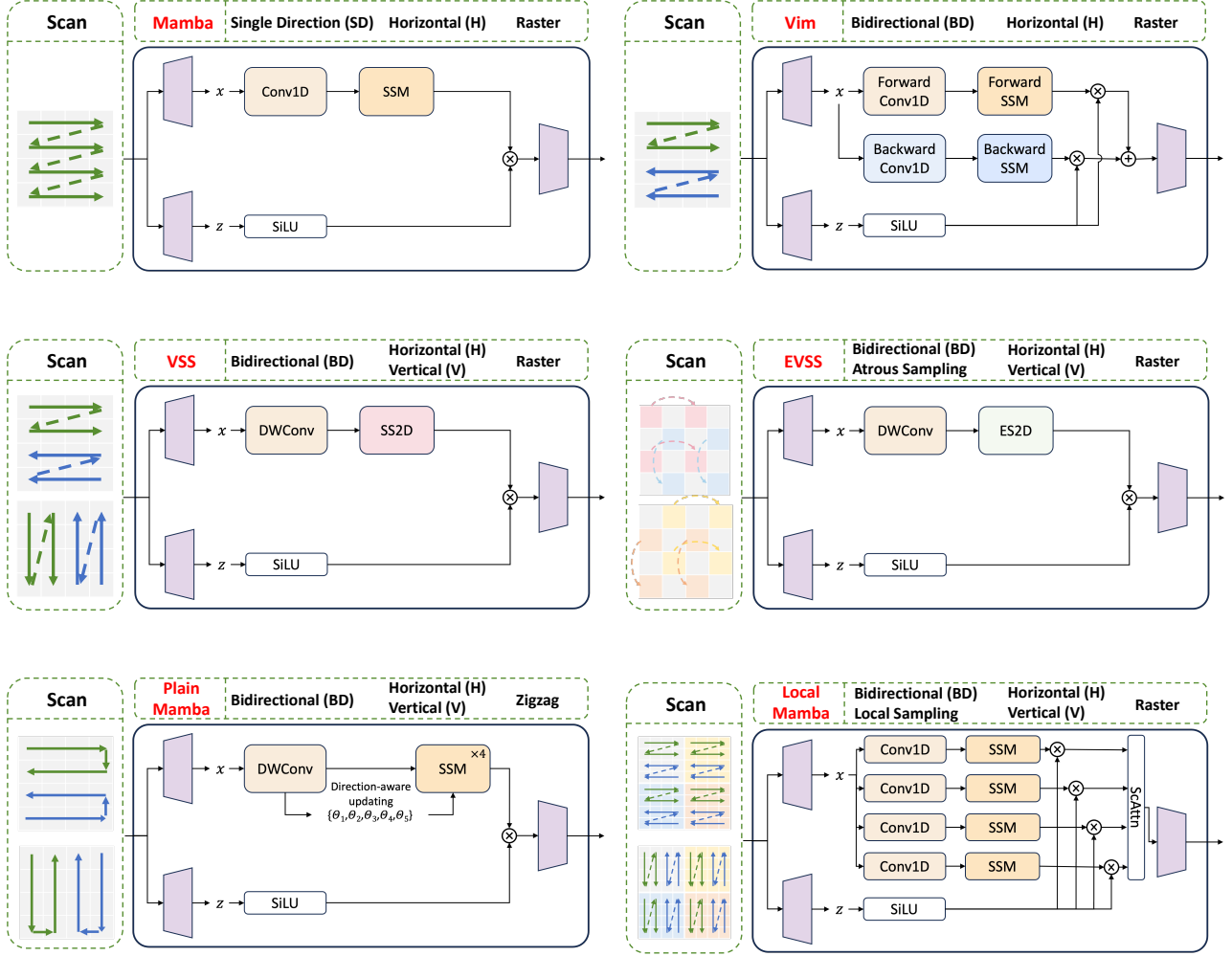


**Fig. 3** Visual Mamba blocks, including Vision Mamba (Vim) (Zhu et al, 2024a), Visual State Space (VSS) (Liu et al, 2024g), Efficient Visual State Space (EVSS) (Pei et al, 2024), PlainMamba (Yang et al, 2024a), and LocalMamba (Huang et al, 2024e) blocks. The original Mamba (Gu and Dao, 2023) block is presented as a reference for the advancements in the visual Mamba blocks. The scan techniques and their decoupling results are displayed to the left and above the corresponding blocks, respectively

Mamba-ND (Li et al, 2024d) aims to extend Mamba to multi-dimensional data including images and videos. It treats the 1D Mamba layer as a black box and explores how to unravel and order multi-dimensional data. Results show that a chain of Mamba layers and simple alternating-directional orderings achieve superior performance. FractalMamba (Tang et al, 2024b) adopts a fractal scanning curve, namely the Hilbert curve, as depicted in Fig. 4, for processing 2D image patches. Differently, Mamba<sup>®</sup> (Wang et al, 2024a) identifies that the feature artifacts observed in vision Transformers are more pronounced in Vim (Zhu et al, 2024a). To alleviate this issue, Mamba<sup>®</sup> refines Vim by strategically

inserting input-independent tokens, referred to as register (Darcet et al, 2024) tokens, into the visual token sequence. ARM (Ren et al, 2024b) demonstrates that autoregressive pre-training is well-suited to the Mamba architecture, significantly enhancing its visual performance and unlocking its scaling potential.

### 3.2 Hybrid Mamba

In addition to standalone usages, several studies have explored the integration of Mamba with other architectural paradigms to construct hybrid Mamba networks.

*LocalMamba*: LocalMamba (Huang et al, 2024e) identifies a significant limitation in the Vim (Zhu et al, 2024a) and VMamba (Liu et al, 2024g) models, the disrupted dependencies among spatially local tokens during a single scanning process. To overcome this issue, as local sampling depicted in Fig. 4, LocalMamba divides the input image into multiple local windows to perform SSM in different directions as VMamba (Liu et al, 2024g), while also maintaining the global SSM operations. Furthermore, LocalMamba implements a spatial and channel attention module before patch merging to enhance the integration of directional features and reduce redundancy. The LocalMamba block is illustrated in Fig. 3. In addition, it adopts a strategy to select the most effective scan directions for each layer, thereby optimizing computational efficiency.

*EfficientVMamba*: EfficientVMamba (Pei et al, 2024) introduces the Efficient 2D Scanning (ES2D) technique, which employs atrous sampling of patches on the feature map to reduce computational burdens. The atrous sampling is illustrated in Fig. 4. ES2D is used to extract the global features, while a parallel convolutional branch is used to extract the local features. Both feature types are then individually processed by a Squeeze-and-Excitation (SE) block. Collectively, the ES2D, the convolutional branch, and the SE block constitute the core components of the Efficient Visual State Space (EVSS) block. The output of the EVSS block is the summation of the modulated global and local features. The EVSS block is shown in Fig. 3. The EVSS blocks form the early stages of the EfficientVMamba, whereas the Inverted Residual blocks (Sandler et al, 2018) invertedly form the later stages.

Some backbone networks introduce the operations from the frequency domain. SiMBA (Patro and Agneewaran, 2024b) aims to address the instability issue of Mamba scaling to large networks on vision datasets. It uses Mamba for sequence modeling and proposes a new channel modeling technique termed Einstein FFT (EinFFT). The EinFFT applies the Fourier Transform and performs Einstein Matrix Multiplication (EMM) in the frequency domain. Specifically, EMM reorganizes the input and the weight matrix along the channel dimensions into blocks, such that each block is a diagonal matrix for efficient computation. After multiplication, a non-linear activation function is applied to modulate the eigenvalues in the Mamba block to ensure stability following the principle that stability is achieved if all eigenvalues of the evolution matrix are negative real numbers (Oppenheim and Verghese, 2010). Vim-F (Zhang et al, 2024b) utilizes the Fourier transform to transfer the feature map into the frequency domain and

adds it to the original feature map, thus mitigating the drawbacks of Vim (Zhu et al, 2024a). Since each point in the frequency feature map depends on the entire original feature map, frequency-domain scanning ensures a comprehensive global receptive field. Moreover, the translation invariance characteristic of the Fourier transform helps to mitigate the inductive bias introduced by the scanning strategy. Vim-F further eliminates the need for position embedding and introduces a new patch embedding method tailored for Mamba, employing overlapping convolutions to model the spatial correlation between tokens. In addition, to balance performance with efficiency, MSVMamba (Shi et al, 2024a) modifies the SS2D scanning used in VMamba (Liu et al, 2024g) by downsampling the image in three directions within SS2D to shorten the sequence length, forming a Multi-Scale 2D (MS2D) scanning strategy. Additionally, each MSVMamba block incorporates a Convolutional Feed-Forward Network (ConvFFN) to enhance channel-wise information exchange and local feature extraction.

### 3.3 Summary of Key Improvements

#### 3.3.1 Tokenization

To process 2D images, they are first converted into sequences of visual tokens via a stem module, typically comprising a convolution layer followed by a linear projection layer. The addition of positional embeddings is optional, as the SSM operation inherently possesses causal properties. The inclusion of a class token is also optional. Some works insert extra tokens to act as register (Darcet et al, 2024) or to perceive discontinuities between rows or columns. Existing approaches process image sequences by treating them as either 1D or 2D structures for the SSM transformations and convolution operations in the Mamba-based blocks. Given the integral role of scanning techniques in these processes, we will systematically categorize and delve into these approaches in detail in the subsequent section.

#### 3.3.2 Scan

The selective scanning mechanism is the key component of Mamba. However, its original design for 1D causal sequences poses challenges when adapting it to non-causal visual data. Considerable research efforts are devoted to addressing these challenges. In the following section, we categorize and discuss these efforts into four main groups: scan direction, scan axis, scan continuity, and scan sampling. This categorization is based on the



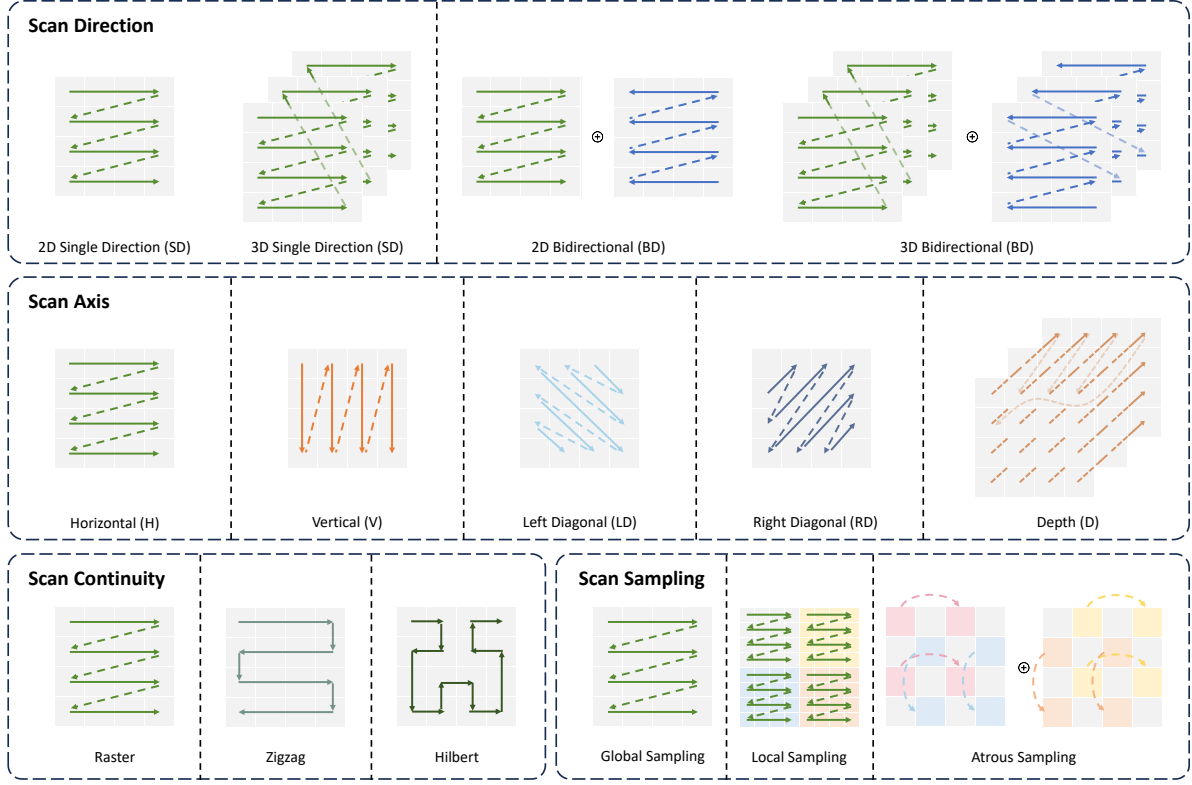


**Fig. 4** Scan techniques, categorized into four groups, i.e., scan direction, scan axis, scan continuity, and scan sampling

objectives of the scanning techniques. The scan direction addresses the non-causal characteristics of visual sequences; the scan axis deals with the high dimensionality inherent in visual data; the scan continuity considers the spatial continuity of the patches along the scanning path; the scan sampling divides the full image into sub-images to capture spatial information. The illustration of these four groups is shown in Fig. 4.

*Scan Direction:* After unfolding the visual data into 1D sequences, different scan directions can be employed to handle the non-causal nature of these sequences. We first denote the original selective scanning technique, which operates in a single direction, as **SD**. In (Zhu et al, 2024a), bi-directional sequence modeling is employed to enhance the receptive fields reciprocally. We refer to this approach as **BD**. In addition to the two common scan directions, supplementary shuffle or re-ordering strategies can be employed for scanning. We denote the utilization of these strategies with the labels **+Shuffle** or **+Reordering**, respectively.

*Scan Axis:* Visual data differ from typical sequences by possessing 2D or higher-dimensional spatial information that encapsulates both local and global con-

texts. Current approaches unfold visual data along various axes to thoroughly integrate this spatial information. For instance, the scanning axes for a 2D image typically include the horizontal, vertical, left diagonal, and right diagonal, designated as **H**, **V**, **LD**, and **RD**, respectively. For 3D visual data, the axes also involve depth or temporal dimensions, denoted as **D**.

*Scan Continuity:* Alternative techniques are employed to handle the 2D spatial information in visual data. Some approaches, inspired by the ViT (Dosovitskiy et al, 2021), flatten images into sequences. This technique, however, may lead to spatial discontinuities between rows or columns; we refer to this technique as **Raster** scanning. In contrast, other approaches ensure continuous scanning to maintain spatial continuity among adjacent tokens, a technique we denote as **Zigzag**. Some approaches utilize fractal scanning curves to better capture the structural information within the image. Specifically, the use of the Hilbert curve, which we refer to as **Hilbert**, preserves their spatial relationships and significantly improves the token adjacency.

*Scan Sampling:* We denote sampling techniques that divide the image into sub-images for scanning as **Local**



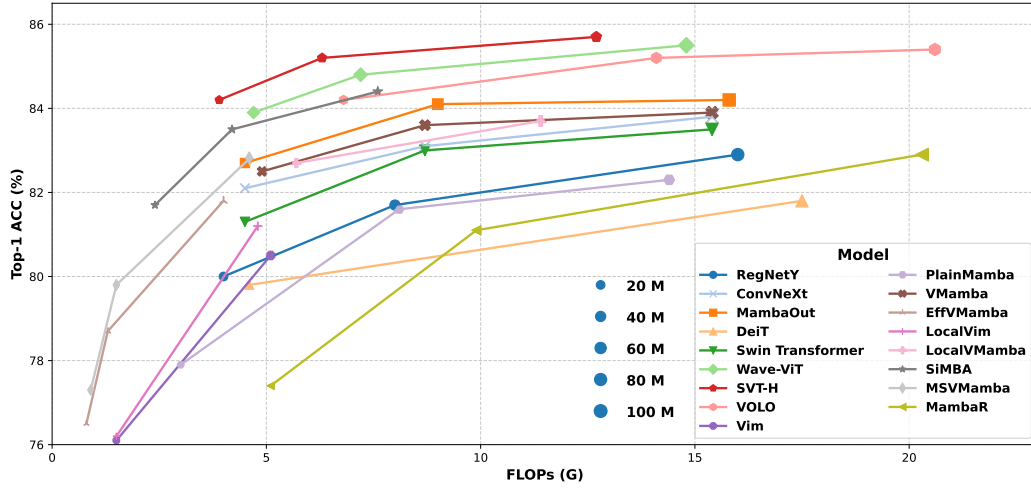


**Fig. 5** Comparative analysis of the performance and computational complexity across various visual backbone architectures, encompassing Convolution-based methods (Radosavovic et al, 2020; Liu et al, 2022b; Yu and Wang, 2024), Transformer-based methods (Touvron et al, 2021; Liu et al, 2021; Yao et al, 2022; Patro and Agneeswaran, 2023; Yuan et al, 2023), and Mamba-based methods (Zhu et al, 2024a; Yang et al, 2024a; Liu et al, 2024g; Pei et al, 2024; Huang et al, 2024e; Chaudhuri and Bhattacharya, 2024; Shi et al, 2024a; Wang et al, 2024a). The symbol size is proportional to the parameter count of respective model, providing a visual indicator of model scale and complexity. Note that all data are accessed from released academic papers to ensure fairness and credibility

**Sampling** and **Atrous Sampling** based on the original terminology in their papers. Notably, within these sub-images, different combinations of the former three groups of scanning techniques can be applied, allowing for diverse processing approaches without the necessity for uniformity across all sub-images. The comparison of the obtained sub-images and the original full image, which is denoted as **Global Sampling**, is illustrated.

These four groups of scanning techniques are interoperable and can be synergistically combined to enhance visual data analysis.

### 3.3.3 Block

Different combinations of the previously mentioned scanning techniques and the selective SSM transformation form various blocks, which are integral to Mamba-based architectures. In discussing the visual Mamba backbone networks, we provide an overview of these blocks. Fig. 3 illustrates a suite of visual Mamba blocks, including Vision Mamba (Vim) (Zhu et al, 2024a), Visual State Space (VSS) (Liu et al, 2024g), Efficient Visual State Space (EVSS) (Pei et al, 2024), PlainMamba (Yang et al, 2024a), and LocalMamba (Huang et al, 2024e) blocks. The Mamba (Gu and Dao, 2023) block is also included to facilitate a direct comparison, highlighting the evolutionary design of these blocks in the visual domain. The detailed illustrations of scanning techniques of different blocks and their

decoupled results presented in Fig. 3 also validate the logic behind our categorization of scanning techniques. Since the Mamba, Vim, and VSS blocks are extensively utilized in the applications that will be detailed in the subsequent section. For clarity, we simply refer to them as **Mamba**, **Vim** and **VSS**. Their algorithmic details are presented in the Online Resource. Modifications to these blocks are indicated by an asterisk (\*).

## 3.4 Experimental Results

In this section, we compare the experimental results of different visual Mamba backbone networks with popular architectures based on CNNs or Transformers on standard computer vision benchmarks.

### 3.4.1 Image Classification

Image classification performance is compared on ImageNet-1K (Deng et al, 2009) and the Top-1 accuracy results from the respective papers are listed in Table. 1. The results are categorized into three groups based on different architectures: CNNs, Transformers, and Mamba-based models. The best, second-best, and third-best results are bolded and distinguished using red, blue, and green, respectively. To clearly compare different networks, we also plot their performance and computational complexity in Fig. 5.

**Table 1** Comparison of different backbones on ImageNet-1K (Deng et al, 2009) classification. \* indicates that the backbone has undergone additional training using the Token Labeling objective (Wang et al, 2022a). † indicates results reproduced by DeiT (Touvron et al, 2021). The **best**, **second-best**, and **third-best** results are bolded and distinguished using red, blue, and green, respectively

Backbone	Image Size	Params	FLOPs	Top-1 ACC
<b>CNNs</b>				
RegNetY-4G <sup>†</sup> (Radosavovic et al, 2020)	224 × 224	20.6 M	4.0 G	80.0
RegNetY-8G <sup>†</sup> (Radosavovic et al, 2020)	224 × 224	39.2 M	8.0 G	81.7
RegNetY-16G <sup>†</sup> (Radosavovic et al, 2020)	224 × 224	83.6 M	16.0 G	82.9
ConvNeXt-T (Liu et al, 2022b)	224 × 224	29.0 M	4.5 G	82.1
ConvNeXt-S (Liu et al, 2022b)	224 × 224	50.0 M	8.7 G	83.1
ConvNeXt-B (Liu et al, 2022b)	224 × 224	89.0 M	15.4 G	<b>83.8</b>
MambaOut-T (Yu and Wang, 2024)	224 × 224	27.0 M	4.5 G	82.7
MambaOut-S (Yu and Wang, 2024)	224 × 224	48.0 M	9.0 G	<b>84.1</b>
MambaOut-B (Yu and Wang, 2024)	224 × 224	85.0 M	15.8 G	<b>84.2</b>
<b>Transformers</b>				
ViT-B/16 (Dosovitskiy et al, 2021)	384 × 384	86.0 M	55.4 G	77.9
ViT-L/16 (Dosovitskiy et al, 2021)	384 × 384	307.0 M	190.7 G	76.5
DeiT-Ti (Touvron et al, 2021)	224 × 224	5.0 M	1.3 G	72.2
DeiT-S (Touvron et al, 2021)	224 × 224	22.0 M	4.6 G	79.8
DeiT-B (Touvron et al, 2021)	224 × 224	86.0 M	17.5 G	81.8
DeiT-B* (Touvron et al, 2021)	384 × 384	86.0 M	55.4 G	83.1
Swin-T (Liu et al, 2021)	224 × 224	29.0 M	4.5 G	81.3
Swin-S (Liu et al, 2021)	224 × 224	50.0 M	8.7 G	83.0
Swin-B (Liu et al, 2021)	224 × 224	88.0 M	15.4 G	83.5
Swin-B* (Liu et al, 2021)	384 × 384	88.0 M	47.0 G	84.5
Wave-ViT-S* (Yao et al, 2022)	224 × 224	22.7 M	4.7 G	83.9
Wave-ViT-B* (Yao et al, 2022)	224 × 224	33.5 M	7.2 G	84.8
Wave-ViT-L* (Yao et al, 2022)	224 × 224	57.5 M	14.8 G	<b>85.5</b>
SVT-H-S* (Patro and Agneeswaran, 2023)	224 × 224	22.0 M	3.9 G	84.2
SVT-H-B* (Patro and Agneeswaran, 2023)	224 × 224	32.8 M	6.3 G	85.2
SVT-H-L* (Patro and Agneeswaran, 2023)	224 × 224	54.0 M	12.7 G	<b>85.7</b>
VOLO-D1* (Yuan et al, 2023)	224 × 224	27.0 M	6.8 G	84.2
VOLO-D2* (Yuan et al, 2023)	224 × 224	59.0 M	14.1 G	85.2
VOLO-D3* (Yuan et al, 2023)	224 × 224	86.0 M	20.6 G	85.4
VOLO-D4* (Yuan et al, 2023)	224 × 224	193.0 M	43.8 G	<b>85.7</b>
VOLO-D5* (Yuan et al, 2023)	224 × 224	296.0 M	69.0 G	<b>86.1</b>
<b>Mambas</b>				
Vim-Ti (Zhu et al, 2024a)	224 × 224	7.0 M	1.5 G	76.1
Vim-S (Zhu et al, 2024a)	224 × 224	26.0 M	5.1 G	80.5
Mamba <sup>®</sup> -T (Wang et al, 2024a)	224 × 224	9.0 M	5.1 G	77.4
Mamba <sup>®</sup> -S (Wang et al, 2024a)	224 × 224	28.0 M	9.9 G	81.1
Mamba <sup>®</sup> -B (Wang et al, 2024a)	224 × 224	99.0 M	20.3 G	82.9
Mamba <sup>®</sup> -L (Wang et al, 2024a)	224 × 224	341.0 M	55.5 G	83.2
PlainMamba-L1 (Yang et al, 2024a)	224 × 224	7.0 M	3.0 G	77.9
PlainMamba-L2 (Yang et al, 2024a)	224 × 224	25.0 M	8.1 G	81.6
PlainMamba-L3 (Yang et al, 2024a)	224 × 224	50.0 M	14.4 G	82.3
Mamba-2D-S (Li et al, 2024d)	224 × 224	24.0 M	-	81.7
Mamba-2D-B (Li et al, 2024d)	224 × 224	92.0 M	-	83.0
VMamba-T (Liu et al, 2024g)	224 × 224	31.0 M	4.9 G	82.5
VMamba-S (Liu et al, 2024g)	224 × 224	50.0 M	8.7 G	83.6
VMamba-B (Liu et al, 2024g)	224 × 224	89.0 M	15.4 G	<b>83.9</b>
FractalMamba-T (Tang et al, 2024b)	224 × 224	31.0 M	4.9 G	82.7
Vim-Ti-F(H) (Zhang et al, 2024b)	224 × 224	7 M	1.5 G	76.0
Vim-S-F(H) (Zhang et al, 2024b)	224 × 224	26 M	5.1 G	80.4
EHFV Mamba-T (Pei et al, 2024)	224 × 224	6.0 M	0.8 G	76.5
EHFV Mamba-S (Pei et al, 2024)	224 × 224	11.0 M	1.3 G	78.7
EHFV Mamba-B (Pei et al, 2024)	224 × 224	33.0 M	4.0 G	81.8
MSVMamba-N (Shi et al, 2024a)	224 × 224	7.0 M	0.9 G	77.3
MSVMamba-M (Shi et al, 2024a)	224 × 224	12.0 M	1.5 G	79.8
MSVMamba-T (Shi et al, 2024a)	224 × 224	33.0 M	4.6 G	82.8
LocalVim-T (Huang et al, 2024e)	224 × 224	8.0 M	1.5 G	76.2
LocalVim-S (Huang et al, 2024e)	224 × 224	28.0 M	4.8 G	81.2
LocalVMamba-T (Huang et al, 2024e)	224 × 224	26.0 M	5.7 G	82.7
LocalVMamba-S (Huang et al, 2024e)	224 × 224	50.0 M	11.4 G	<b>83.7</b>
SIMBA-S (Patro and Agneeswaran, 2024b)	224 × 224	15.3 M	2.4 G	81.7
SIMBA-B (Patro and Agneeswaran, 2024b)	224 × 224	22.8 M	4.2 G	83.5
SIMBA-L (Patro and Agneeswaran, 2024b)	224 × 224	36.6 M	7.6 G	<b>84.4</b>

As seen, the performance of all the models improves as model sizes increase, illustrating the trend of enhancing performance through model scaling. It is evident that with similar computational complexity, most visual Mamba networks outperform the CNN-based RegNetY (Radosavovic et al, 2020) and the Transformer-based DeiT (Touvron et al, 2021). Furthermore, VMamba (Liu et al, 2024g), LocalVMamba (Huang et al, 2024e), and SiMBA (Chaudhuri and Bhattacharya, 2024) all surpass the CNN-based Con-

**Table 2** Results of object detection and instance segmentation on MS COCO (Lin et al, 2014) *mini-val* using Mask R-CNN (He et al, 2017) 1× schedule. FLOPs are computed using an input size 1280×800. † indicates FLOPs computed using an input size 1333×800. The **best**, **second-best**, and **third-best** results are bolded and distinguished using red, blue, and green, respectively

Backbone	Params	FLOPs	AP <sup>b</sup>	AP <sup>b</sup> <sub>50</sub>	AP <sup>b</sup> <sub>75</sub>	AP <sup>m</sup>	AP <sup>m</sup> <sub>50</sub>	AP <sup>m</sup> <sub>75</sub>
<b>CNNs</b>								
ConvNeXt-T (Liu et al, 2022b)	48.0 M	262.0 G	44.2	66.6	48.3	40.1	63.3	42.8
ConvNeXt-S (Liu et al, 2022b)	70.0 M	348.0 G	<b>45.4</b>	67.9	50.0	<b>41.8</b>	65.2	45.1
MambaOut-T (Yu and Wang, 2024)	43.0 M	262.0 G	<b>45.1</b>	67.3	49.6	41.0	64.1	44.1
MambaOut-S (Yu and Wang, 2024)	65.0 M	354.0 G	<b>47.4</b>	69.1	52.4	<b>42.7</b>	66.1	46.2
MambaOut-B (Yu and Wang, 2024)	100.0 M	495.0 G	<b>47.4</b>	69.3	52.2	<b>43.0</b>	66.4	46.3
<b>Transformers</b>								
ViT-Adpt-T (Chen et al, 2023)	28.1 M	-	41.1	62.5	44.3	37.5	59.7	39.9
ViT-Adpt-S (Chen et al, 2023)	47.8 M	-	44.7	65.8	48.3	39.9	62.5	42.8
ViT-Adpt-B (Chen et al, 2023)	120.2 M	-	47.0	68.2	51.4	41.8	65.1	44.9
Swin-T (Liu et al, 2021)	48.0 M	264.0 G	42.2	-	-	39.1	-	-
Swin-S (Liu et al, 2021)	69.0 M	354.0 G	44.8	-	-	40.9	-	-
Swin-B (Liu et al, 2021)	107.0 M	496.0 G	46.9	-	-	42.3	-	-
PVTv2-B2 (Wang et al, 2022b)	45.0 M	-	45.3	67.1	49.6	41.2	64.2	44.4
PVTv2-B3 (Wang et al, 2022b)	64.9 M	-	47.0	68.1	51.7	42.5	65.7	45.7
PVTv2-B4 (Wang et al, 2022b)	82.2 M	-	47.5	68.7	52.0	42.7	66.1	46.1
PVTv2-B5 (Wang et al, 2022b)	101.6 M	-	47.4	68.6	51.9	42.5	65.7	46.0
ViL-T <sup>†</sup> (Zhang et al, 2021)	26.9 M	145.6 G	41.4	63.5	45.0	38.1	60.3	40.8
ViL-S <sup>†</sup> (Zhang et al, 2021)	45.0 M	218.3 G	44.9	67.1	49.3	41.0	64.2	44.1
ViL-M <sup>†</sup> (Zhang et al, 2021)	60.1 M	293.8 G	47.6	69.8	52.1	<b>43.0</b>	66.9	46.6
ViL-B <sup>†</sup> (Zhang et al, 2021)	76.1 M	384.4 G	<b>48.6</b>	70.5	53.4	<b>43.6</b>	67.6	47.1
SG-Former-S (Ren et al, 2023)	41.0 M	-	47.4	69.0	52.0	42.6	65.9	46.0
SG-Former-M (Ren et al, 2023)	51.0 M	-	<b>48.2</b>	70.3	53.1	<b>43.6</b>	66.9	47.0
SG-Former-B (Ren et al, 2023)	95.0 M	-	<b>49.2</b>	70.6	54.3	<b>43.2</b>	68.1	47.7
<b>Mambas</b>								
PlainMamba-L1 (Yang et al, 2024a)	31.0 M	388.0 G	44.1	64.8	47.9	39.1	61.6	41.9
PlainMamba-L2 (Yang et al, 2024a)	53.0 M	542.0 G	46.0	66.9	50.1	40.6	63.8	43.6
PlainMamba-L3 (Yang et al, 2024a)	79.0 M	696.0 G	46.8	68.0	51.1	41.2	64.7	43.9
VMamba-T (Liu et al, 2024g)	50.0 M	270.0 G	47.4	69.5	52.0	42.7	66.3	46.0
VMamba-S (Liu et al, 2024g)	64.0 M	357.0 G	<b>48.7</b>	70.0	53.4	<b>43.7</b>	67.3	47.0
VMamba-B (Liu et al, 2024g)	108.0 M	485.0 G	<b>49.2</b>	70.9	53.9	<b>43.9</b>	67.7	47.6
FractalMamba-T (Tang et al, 2024b)	50.0 M	270.0 G	47.8	70.0	52.4	42.9	66.6	46.3
EHFV Mamba-T (Pei et al, 2024)	11.0 M	60.0 G	35.6	57.7	38.0	33.2	54.4	35.1
EHFV Mamba-S (Pei et al, 2024)	31.0 M	197.0 G	39.3	61.8	42.6	36.7	58.9	39.2
EHFV Mamba-B (Pei et al, 2024)	53.0 M	252.0 G	43.7	66.2	47.9	40.2	63.3	42.9
MSVMamba-M (Shi et al, 2024a)	32.0 M	201.0 G	43.8	65.8	47.7	39.9	62.9	42.9
MSVMamba-T (Shi et al, 2024a)	53.0 M	252.0 G	46.9	68.8	51.4	42.2	65.6	45.4
LocalVMamba-T (Huang et al, 2024e)	45.0 M	291.0 G	46.7	68.7	50.8	42.2	65.7	45.5
LocalVMamba-S (Huang et al, 2024e)	69.0 M	414.0 G	<b>48.4</b>	69.9	52.7	<b>43.2</b>	66.7	46.5
SIMBA-S (Patro and Agneeswaran, 2024b)	60.0 M	382.0 G	46.9	68.6	51.7	42.6	65.9	45.8

vNeXt (Liu et al, 2022b) and Transformer-based Swin Transformer (Liu et al, 2021). These results demonstrate the superior performance of visual Mamba networks compared to common CNNs and Transformers. Although CNN-based MambaOut (Yu and Wang, 2024) outperforms most visual Mamba networks, it does not exceed the performance of the Mamba-based SiMBA (Patro and Agneeswaran, 2024b). Additionally, Transformer-based networks are highly competitive, particularly SVT (Patro and Agneeswaran, 2023), Wave-ViT (Yao et al, 2022), and VOLO (Yuan et al, 2023), which consistently demonstrate superior performance over other networks. Notably, VOLO (Yuan et al, 2023) also exhibits excellent scalability.

Currently, despite their efficiency, most Mamba-based networks are limited to small-scale implementations with FLOPs under 21G. While Mamba<sup>®</sup> has demonstrated scalability to larger models, there remains a need for performance enhancements. To sum up, visual Mamba networks exhibit promising performance but still underperform advanced CNN- and Transformer-based networks. Further exploration is also needed to scale visual Mamba networks to larger configurations.

**Table 3** Results of semantic segmentation on ADE20K (Zhou et al, 2019) *val* using UperNet (Xiao et al, 2018). FLOPs are calculated using an input size  $512 \times 2048$ . ‘SS’ and ‘MS’ denote single-scale and multi-scale testing, respectively. MLN: multi-level neck. The **best**, **second-best**, and **third-best** results are bolded and distinguished using red, blue, and green, respectively

Backbone	Crop Size	Params	FLOPs	mIoU (SS)	mIoU (MS)
<b>CNNs</b>					
ConvNeXt-T (Liu et al, 2022b)	$512 \times 512$	60.0 M	939.0 G	46.0	46.7
ConvNeXt-S (Liu et al, 2022b)	$512 \times 512$	82.0 M	1027.0 G	48.7	49.6
ConvNeXt-B (Liu et al, 2022b)	$512 \times 512$	122.0 M	1170.0 G	<b>49.1</b>	<b>49.9</b>
MambaOut-T (Yu and Wang, 2024)	$512 \times 512$	54.0 M	938.0 G	47.4	48.6
MambaOut-S (Yu and Wang, 2024)	$512 \times 512$	76.0 M	1032.0 G	<b>49.5</b>	<b>50.6</b>
MambaOut-B (Yu and Wang, 2024)	$512 \times 512$	112.0 M	1178.0 G	<b>49.6</b>	<b>51.0</b>
<b>Transformers</b>					
ViT-Adpt-T (Chen et al, 2023)	$512 \times 512$	36.1 M	-	42.6	43.6
ViT-Adpt-S (Chen et al, 2023)	$512 \times 512$	57.6 M	-	46.2	47.1
ViT-Adpt-B (Chen et al, 2023)	$512 \times 512$	133.9 M	-	48.8	49.7
DeiT-S + MLN (Touvron et al, 2022)	$512 \times 512$	58.0 M	1217.0 G	43.8	45.1
DeiT-B + MLN (Touvron et al, 2022)	$512 \times 512$	144.0 M	2007.0 G	45.5	47.2
Swin-T (Liu et al, 2021)	$512 \times 512$	60.0 M	945.0 G	44.4	45.8
Swin-S (Liu et al, 2021)	$512 \times 512$	81.0 M	1039.0 G	47.6	49.5
Swin-B (Liu et al, 2021)	$512 \times 512$	121.0 M	1188.0 G	48.1	49.7
SG-Former-S (Ren et al, 2023)	$512 \times 512$	52.5 M	989.0 G	<b>49.9</b>	<b>51.5</b>
SG-Former-M (Ren et al, 2023)	$512 \times 512$	68.3 M	1114.0 G	<b>51.2</b>	<b>52.1</b>
SG-Former-B (Ren et al, 2023)	$512 \times 512$	109.3 M	1304.0 G	<b>52.0</b>	<b>52.7</b>
<b>Mambas</b>					
Vim-Ti (Zhu et al, 2024a)	$512 \times 512$	13.0 M	-	41.0	-
Vim-S (Zhu et al, 2024a)	$512 \times 512$	46.0 M	-	44.9	-
Mamba <sup>®</sup> -S (Wang et al, 2024a)	$512 \times 512$	56.0 M	-	45.3	-
Mamba <sup>®</sup> -B (Wang et al, 2024a)	$512 \times 512$	132.0 M	-	47.7	-
Mamba <sup>®</sup> -L (Wang et al, 2024a)	$512 \times 512$	377.0 M	-	49.1	-
PlainMamba-L1 (Yang et al, 2024a)	$512 \times 512$	35.0 M	174.0 G	44.1	-
PlainMamba-L2 (Yang et al, 2024a)	$512 \times 512$	55.0 M	285.0 G	46.8	-
PlainMamba-L3 (Yang et al, 2024a)	$512 \times 512$	81.0 M	419.0 G	49.1	-
VMamba-T (Liu et al, 2024g)	$512 \times 512$	62.0 M	948.0 G	48.3	48.6
VMamba-S (Liu et al, 2024g)	$512 \times 512$	82.0 M	1039.0 G	<b>50.6</b>	<b>51.2</b>
VMamba-B (Liu et al, 2024g)	$512 \times 512$	122.0 M	1170.0 G	<b>51.0</b>	<b>51.6</b>
FractalMamba-T (Tang et al, 2024b)	$512 \times 512$	62.0 M	948.0 G	48.9	49.8
EHVMamba-T (Pei et al, 2024)	$512 \times 512$	14.0 M	230.0 G	38.9	39.3
EHVMamba-S (Pei et al, 2024)	$512 \times 512$	29.0 M	505.0 G	41.5	42.1
EHVMamba-B (Pei et al, 2024)	$512 \times 512$	65.0 M	930.0 G	46.5	47.3
MSVMamba-B (Shi et al, 2024a)	$512 \times 512$	42.0 M	875.0 G	45.1	45.4
MSVMamba-T (Shi et al, 2024a)	$512 \times 512$	65.0 M	942.0 G	47.6	48.5
LocalVim-T (Huang et al, 2024e)	$512 \times 512$	36.0 M	181.0 G	43.4	44.4
LocalVim-S (Huang et al, 2024e)	$512 \times 512$	58.0 M	297.0 G	46.4	47.5
LocalVMamba-T (Huang et al, 2024e)	$512 \times 512$	57.0 M	970.0 G	47.9	49.1
LocalVMamba-S (Huang et al, 2024e)	$512 \times 512$	81.0 M	1095.0 G	<b>50.0</b>	<b>51.0</b>
SiMBA-S (Patro and Agneeswaran, 2024b)	$512 \times 512$	62.0 M	1040.0 G	49.0	49.6

### 3.4.2 Object Detection

Object detection and instance segmentation performance are compared on the MS COCO (Lin et al, 2014) via Mask R-CNN (He et al, 2017) and the results from the respective papers are listed in Table. 2.

The object detection and instance segmentation performance of all the models follows the scaling law as well. It can be observed that with comparable computational complexity, visual Mamba networks surpass the CNN-based ConvNeXt (Liu et al, 2022b), except for EfficientVMamba (Pei et al, 2024), which is designed for lightweight purposes. The performance of VMamba (Liu et al, 2024g) is the best among the visual Mamba networks. VMamba (Liu et al, 2024g) outperforms all the CNN-based networks and most Transformer-based networks. However, its performance is slightly worse than that of SG-Former (Ren et al, 2023).

These results demonstrate that Mamba’s ability to capture long-range dependencies and utilize dynamic weights is advantageous for dense prediction tasks. However, its selection mechanism may limit its performance compared to Transformer-based approaches. Nevertheless, visual Mamba networks show significant

potential in object detection and instance segmentation. Currently, Mamba-based models are not specifically tailored for these tasks, indicating potential for future research to explore and enhance their performance.

### 3.4.3 Semantic Segmentation

Semantic segmentation performance is compared on ADE20K (Zhou et al, 2019) utilizing UperNet (Xiao et al, 2018) and the results from the respective papers are listed in Table. 3.

The semantic segmentation performance of different networks is similar to their object detection performance. VMamba (Liu et al, 2024g) performs the best among the visual Mamba networks, surpassing all CNN-based networks and most Transformer-based networks. However, its performance lags behind that of SG-Former (Ren et al, 2023). These results further demonstrate Mamba’s efficacy in dense prediction tasks. Further exploration of Mamba-based models specifically designed for these tasks is warranted.

In conclusion, Mamba-based models demonstrate adherence to scaling laws. Their advantages are evident in their efficiency and performance in dense prediction tasks, indicating their potential as next-generation visual networks. However, scaling visual Mamba to larger configurations requires further investigation. Additionally, there remains a need for more exploration of Mamba-based models specifically tailored for dense prediction tasks.

## 4 Application

In this section, we systematically categorize and discuss the diverse vision applications of Mamba. The categorization scheme, along with an overview of the reviewed literature in this survey, is presented in Fig. 6.

### 4.1 Image

#### 4.1.1 Classification

In addition to the backbones (Liu et al, 2024g; Zhu et al, 2024a) conducting image classification for representation learning, the scalability of Mamba-based architectures to long sequences has led to their adoption in the analysis of high-dimensional images (e.g., Whole Slide Images, 3D Medical Images and Remote Sensing Images). For instance, MamMIL (Fang et al, 2024) and MambaMIL (Yang et al, 2024c) utilized Mamba to enhance Multiple Instance Learning (MIL) for histopathology image analysis. MamMIL employed

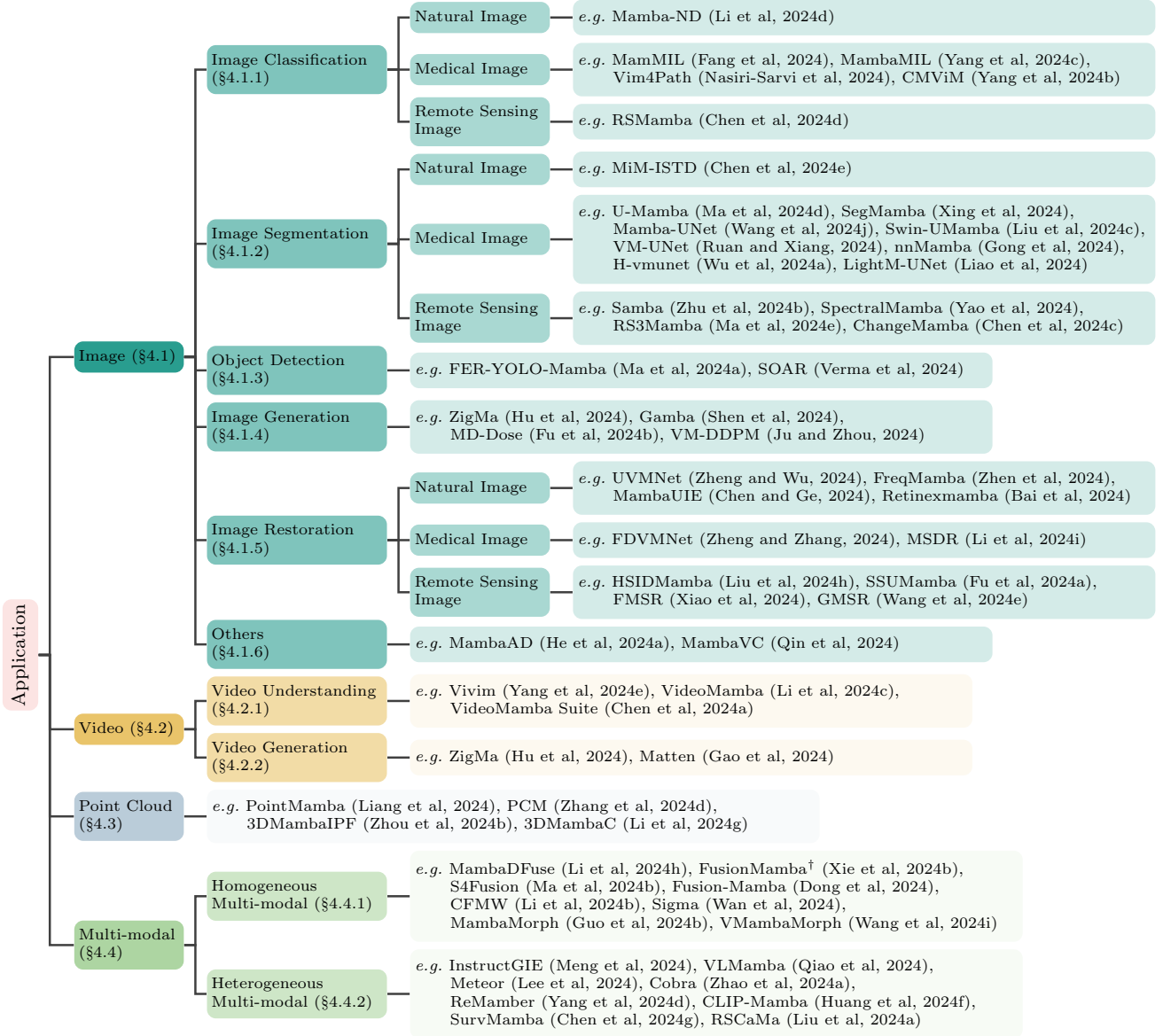


**Fig. 6** The main content flow and categorization of the application in this survey

a bidirectional state space model similar to Vim and a 2D context-aware block (Shao et al, 2021) to enhance instance aggregation. MambaMIL introduced a new approach named Sequence Reordering Mamba (SR-Mamba), which is sensitive to the order and distribution of instances and leverages the valuable information embedded within these long sequences. Differently, Vim4Path (Nasiri-Sarvi et al, 2024) utilized Vim architecture within the DINO (Caron et al, 2021) framework for representation learning. CMViM (Yang et al, 2024b) proposed a contrastive masked Vim autoencoder tailored for 3D multi-modal data to facilitate Alzheimer’s disease (AD) recognition. Other medical image classification methods incorporated the Mamba architecture

with convolutions (Gong et al, 2024; Yue and Li, 2024), channel scanning techniques (Gong et al, 2024), and multi-view fusion (Yang et al, 2024f).

In the remote sensing scenario, RSMamba (Chen et al, 2024d) introduced a position-sensitive dynamic multi-path activation mechanism, encompassing forward, backward, and shuffle paths, to extract precise semantic cues for accurate scene discrimination.

InsectMamba (Wang et al, 2024d) integrated SSMs with convolutions, multi-head self-attention mechanisms, and multilayer perceptions to synergistically leverage the strengths of each encoding strategy for insect pest classification.



**Table 4** The Mamba-based methods in image-level vision tasks (Part I). The abbreviations of Block here are VSS: Vision State Space Module, Vim: Vision Mamba, \*: modification, FT: Fourier Transform. The abbreviations of Data here are CBCT: Cone Beam Computed Tomography, CXR: Chest X-Ray, CT: Computed Tomography, Derm: Dermatoscope, Echo: Echocardiograms, Endo: Endoscopic Images, FMRI: Fast Magnetic Resonance Imaging, Micro: Microscopy Images, MRI: Magnetic Resonance Imaging, OCT: Optical Coherence Tomography, Path: Pathology, PET: Positron Emission Tomography, Skin: Skin Lesion Images, Spleen: Spleen Images, SVCT: Sparse-view Computed Tomography, UI: Ultrasound Images, ODT: Optical Doppler Tomography, HSI: Hyperspectral Images. The abbreviations of Task here are CLS: Classification, DET: Detection, SEG: Segmentation

Methods	Block	Data	Task	Scan	Continuity	Code
<b>Image Classification</b>						
InsectMamba (Wang et al, 2024d)	Mamba*	Natural Images	Insect Pests CLS	SD (H)	Raster	
MamMIL (Fang et al, 2024)	Vim*	Whole Slide Images	Cancer Subtyping	BD (H)	Raster	
MambaMIL (Yang et al, 2024c)	Mamba*	Whole Slide Images	Cancer Subtyping/Survival Prediction	SD (H) + Reordering	Raster	✓
Vim4Path (Nasiri-Sarvi et al, 2024)	Vim	Whole Slide Images	Cancer Subtyping	BD (H)	Raster	✓
CMVIM (Yang et al, 2024b)	Vim	3D Medical Images (MRI & PET)	3D Medical Image CLS	BD (H)	Raster	✓
nnMamba (Gong et al, 2024)	Mamba*	3D Medical Images (CT/MRI)	3D Medical Image CLS	BD (H) + Channel	Raster	✓
MedMamba (Yue and Li, 2024)	VSS*	2D Medical Images (Skin/UI/CXR/Endo/OCT/CT/Micro/Path/Derm)	2D Medical Image CLS	BD (H/V)	Raster	✓
BI-Mamba (Yang et al, 2024f)	Vim	2D Medical Images (X-ray)	Risk Prediction	BD (H)	Raster	✓
RS-Mamba (Chen et al, 2024d)	Mamba	Remote Sensing Images	Remote Sensing Images CLS	BD (H/V) + Shuffle	Raster	✓
<b>Image Segmentation</b>						
MIM-ISTD (Chen et al, 2024e)	VSS*	Infrared Images	Infrared Image SEG	BD (H/W)	Raster	✓
U-Mamba (Ma et al, 2024d)	Mamba*	2D/3D Medical Images (Endo/Micro/CT/MRI)	2D/3D Medical Image SEG	SD (H)	Raster	✓
SegMamba (Xing et al, 2024)	Mamba*	3D Medical Images (CT/MRI)	3D Medical Image SEG	BD (H) + SD (D)	Raster	✓
VM-UNet (Ruan and Xiang, 2024)	VSS	2D Medical Images (Skin/CT)	2D Medical Image SEG	BD (H/V)	Raster	✓
Swin-UMamba (Liu et al, 2024c)	VSS	2D Medical Images (Endo/Micro/MRI)	2D Medical Image SEG	BD (H/V)	Raster	✓
nnMamba (Gong et al, 2024)	Mamba*	3D Medical Images (CT/MRI)	3D Medical Images SEG/Landmark DET	BD (H) + Channel	Raster	✓
Mamba-UNet (Wang et al, 2024j)	VSS	2D Medical Images (CT/MRI)	2D Medical Image SEG	BD (H/V)	Raster	✓
Mamba-ND (Li et al, 2024d)	Mamba*	3D Medical Images (CT)	3D Medical Images SEG	BD (H/V/D)	Raster	✓
Semi-Mamba-UNet (Ma and Wang, 2024)	VSS	2D Medical Images (MRI)	2D Medical Image SEG	BD (H/V)	Raster	✓
P-Mamba (Ye and Chen, 2024)	Vim	2D Medical Images (Echo)	2D Medical Image SEG	BD (H)	Raster	✓
Weak-Mamba-UNet (Wang and Ma, 2024)	VSS	2D Medical Images (MRI)	2D Medical Image SEG	BD (H/V)	Raster	✓
LightM-UNet (Liao et al, 2024)	VSS	2D/3D Medical Images (CXR/CT)	2D/3D Medical Image SEG	BD (H/W)	Raster	✓
LW-Mamba-UNet (Wang et al, 2024c)	Vim*	2D/3D Medical Images (CT/MRI)	2D/3D Medical Image SEG	BD (H)	Raster	✓
VM-UNet-V2 (Zhang et al, 2024c)	VSS	2D Medical Images (Skin/Endo)	2D Medical Image SEG	BD (H/V)	Raster	✓
H-vmmnet (Wu et al, 2024a)	VSS*	2D Medical Images (Skin/Spleen/Endo)	2D Medical Image SEG	BD (H/V)	Raster	✓
ProMamba (Xie et al, 2024a)	Vim	2D Medical Images (Endo)	2D Medical Image SEG	BD (H)	Raster	✓
TM-UNet (Tang et al, 2024a)	VSS*	2D Medical Images (Endo/Micro/CT/MRI)	2D Medical Image SEG	BD (H/V)	Raster	✓
Mamba-HUNet (Sanjid et al, 2024a)	VSS	2D Medical Images (MRI)	2D Medical Image SEG	BD (H/V)	Raster	✓
UltraLight VM-UNet (Wu et al, 2024b)	VSS*	2D Medical Images (Skin)	2D Medical Image SEG	BD (H/V)	Raster	✓
T-Mamba (Hao et al, 2024)	Vim*	3D Medical Images (CBCT)	3D Medical Image SEG	BD (H) + FT	Raster	✓
ViM-UNet (Archit and Pape, 2024)	Vim	2D Medical Images (Cell/Neurite)	2D Medical Images SEG	BD (H)	Raster	✓
nnU-Net Revisited (Isensee et al, 2024)	Mamba*	3D Medical Images (CT/MRI)	3D Medical Images SEG	SD (H)	Raster	✓
Mamba-AHNet (Sanjid et al, 2024b)	VSS*	2D Medical Images (CT)	2D Medical Images SEG	BD (H/V)	Raster	✓
AC-MambaSeg (Nguyen et al, 2024)	VSS*	2D Medical Images (Skin)	2D Medical Images SEG	BD (H/V)	Raster	✓
HC-Mamba (Xu, 2024)	VSS*	2D Medical Images (Skin/CT)	2D Medical Images SEG	BD (H/V)	Raster	✓
MUCM-Net (Yuan et al, 2024)	Mamba	2D Medical Images (Skin)	2D Medical Image SEG	SD (H)	Raster	✓
UU-Mamba (Tsai et al, 2024)	Mamba	2D Medical Images (MRI)	2D Medical Image SEG	SD (H)	Raster	✓
TokenUnify (Chen et al, 2024f)	Mamba	3D Medical Images (Micro)	3D Medical Image SEG	SD (H)	Raster	✓
Samba (Zhu et al, 2024b)	Mamba*	Remote Sensing Images	Semantic SEG	SD (H)	Raster	✓
RS3Mamba (Ma et al, 2024e)	VSS	Remote Sensing Images	Semantic SEG	BD (H/V)	Raster	✓
SpectralMamba (Yao et al, 2024)	Mamba*	Remote Sensing Images	Semantic SEG	SD (H)	Raster	✓
S <sup>2</sup> Mamba (Wang et al, 2024b)	Mamba*	Remote Sensing Images	Semantic SEG	BD (H/V)	Raster	✓
SS-Mamba (Huang et al, 2024d)	Mamba	Remote Sensing Images	Semantic SEG	SD (H)	Raster	✓
Experimental Mamba (Zhu et al, 2024c)	VSS*	Remote Sensing Images	Semantic SEG	BD (H/V/LD/RD)	Raster/Zigzag	✓
CM-UNet (Liu et al, 2024e)	VSS*	Remote Sensing Images	Semantic SEG	BD (H/V)	Raster	✓
RS-Mamba (Zhao et al, 2024b)	Mamba*	Remote Sensing Images	Semantic SEG/Change DET	BD (H/V/LD/RD)	Raster	✓
ChangeMamba (Chen et al, 2024c)	VSS	Remote Sensing Images	Change DET/Building Damage Assessment	BD (H/V)	Raster	✓
Mamba-in-Mamba (Zhou et al, 2024c)	VSS*	Remote Sensing Images	Remote Sensing Images CLS	H/V/H*/V*	Zigzag	✓
3DSS-Mamba (He et al, 2024c)	Mamba*	Remote Sensing Images	Remote Sensing Images CLS	H/V	Raster	✓

#### 4.1.2 Segmentation

Segmentation remains a vital and prominent area in computer vision, holding immense value for diverse real-world applications. Mamba is poised to enhance segmentation tasks due to its capabilities in managing extensive visual data.

MIM-ISTD (Chen et al, 2024e) introduced a novel Mamba-in-Mamba structure, where it employs Outer Mamba to explore the global information and utilizes Inner Mamba to further explore the local information within each visual patch.

Recent advances based on Mamba have appeared in the medical domain, encompassing diverse 2D and 3D medical image datasets Tsai et al (2024); Chen et al (2024f). Several methods (Liu et al, 2024c; Ruan and Xiang, 2024; Ma and Wang, 2024; Wang et al, 2024j;

Sanjid et al, 2024a) directly replace CNN-blocks in the U-Net architecture with Mamba-like blocks (Gu and Dao, 2023; Liu et al, 2024g; Zhu et al, 2024a). U-Mamba (Ma et al, 2024d) is the first effective attempt to apply Mamba in medical image segmentation. It introduced a hybrid CNN-SSM block. SegMamba (Xing et al, 2024) introduced the Gated Spatial Convolution and Tri-orientated Spatial Mamba, which utilized an inter-slice path for 3D data. VM-UNet (Ruan and Xiang, 2024), VM-UNet-V2 Zhang et al (2024c), Swin-UMamba (Liu et al, 2024c), Mamba-UNet (Wang et al, 2024j), Mamba-HUNet (Sanjid et al, 2024a), Mamba-Ahnet (Sanjid et al, 2024b), Ac-mambaseg (Nguyen et al, 2024) and HC-Mamba (Xu, 2024) employed VSS as a basic block to capture extensive contextual information. Mamba-UNet (Wang

et al, 2024j) was further enhanced through the incorporation of semi-supervised (Ma and Wang, 2024) and weak-supervised settings (Wang and Ma, 2024). P-Mamba (Ye and Chen, 2024), ViM-UNet (Archit and Pape, 2024), LW-Mamba-UNet (Wang et al, 2024c), Pro-Mamba (Xie et al, 2024a), T-Mamba (Hao et al, 2024), TM-UNet (Tang et al, 2024a), UltraLight VM-UNet Wu et al (2024b), and MUCM-Net Yuan et al (2024) employed Mamba-like architecture as a basic block with additional designs for enhancement. Meanwhile, some of these Mamba-based methods (Ma et al, 2024d; Ruan and Xiang, 2024; Liu et al, 2024c; Liao et al, 2024; Wang et al, 2024c; Wu et al, 2024a) conducted extensive experiments on both 2D and 3D medical datasets, which demonstrates the efficacy of Mamba architecture for both 2D and 3D medical images. However, (Isensee et al, 2024) noticed validation pitfalls in medical image segmentation. To avoid these pitfalls, a thorough and comprehensive benchmarking of segmentation methods, including CNN-based, Transformer-based, and Mamba-based approaches, was conducted. The results reveal that most methods introduced in recent years fail to surpass the original nnU-Net baseline (Isensee et al, 2018). This motivates us to think about the principle of Mamba compared to CNN and Transformer, and pay more attention to stringent validation standards.

In the field of remote sensing images, Mamba-based approaches typically leverage its efficiency for processing high-resolution images (Zhu et al, 2024b; Ma et al, 2024e; Liu et al, 2024e) and exploit the spatial-spectral characteristics of images to perform scanning (Wang et al, 2024b; Huang et al, 2024d; He et al, 2024c). SpectralMamba (Yao et al, 2024) proposed gated spatial-spectral merging and piece-wise sequential scanning. Mamba-in-Mamba (Zhou et al, 2024c) proposed a centralized Mamba Cross-Scan (MCS) mechanism with a tokenized Mamba to enhance representative feature generation and concentration. ChangeMamba (Chen et al, 2024c) adopted the VSS architecture as the encoder and spatial-temporal relationship modeling mechanisms to achieve spatial-temporal interaction of multi-temporal features. RS-Mamba (Zhao et al, 2024b) introduced an Omni-directional Selective Scan Module based on Mamba. Regarding various scanning strategies adopted in these works, (Zhu et al, 2024c) conducted a comparative study to evaluate the impact of 22 scanning strategies in Mamba-based methods on semantic segmentation of remote sensing images. The findings indicate that these strategies do not significantly enhance performance in this task, raising questions about the effectiveness of multi-directional scanning approaches.

#### 4.1.3 Detection

The advantages of Mamba in extracting global information and performing efficient computations make it particularly well-suited for object detection tasks.

FER-YOLO-Mamba (Ma et al, 2024a) is the first Mamba-based model for facial expression detection. It introduced a dual-branch structure that incorporated omnidirectional Mamba and attention mechanisms for the Feature Pyramid Network (FPN). VMambaCC (Ma et al, 2024c) is a pioneering work that applied the Mamba architecture to crowd counting tasks. It used VSS blocks for feature extraction and combined VSS blocks with attention mechanisms for feature fusion. SOAR (Verma et al, 2024) integrated vision Mamba block, which utilizes position embedding and bidirectional Mamba for effective visual modeling, into the YOLO v9 architecture. This integration enhances the real-time detection performance of small aerial objects.

#### 4.1.4 Generation

Intuitively, applying the Mamba architecture to a series of generation tasks to achieve sufficient long sequence interactions has the potential to achieve impressive performance.

DiS (Fei et al, 2024) leverages a state space-based architectural backbone and treats all inputs, including time, condition and noisy image patches, as tokens, which enables the model to effectively capture long-range dependencies within the data. It achieves compared performance in both unconditional and class-conditional image generation scenarios. ZigMa (Hu et al, 2024) and DiM<sup>†</sup> (Mo and Tian, 2024) are DiT-style (Peebles and Xie, 2023) Mamba diffusion models. Additionally, ZigMa (Hu et al, 2024) leveraged spatial continuity to maximally incorporate the inductive bias from visual data. DiM (Teng et al, 2024) was another diffusion Mamba model specifically designed for efficient high-resolution image synthesis. The authors implemented multi-directional scans to adapt Mamba for 2D signal processing. Furthermore, they introduced learnable padding tokens at the end of each row and column to enhance the model's sensitivity to discontinuities between rows or columns, along with lightweight local feature enhancement. Gamba (Shen et al, 2024) introduced GambaFormer to process 3D Gaussian Splatting by utilizing the newly proposed Gaussian Mamba.

MD-Dose (Fu et al, 2024b) introduced a novel diffusion model based on the Mamba architecture for predicting radiation therapy dose distribution in thoracic cancer patients. VM-DDPM (Ju and Zhou, 2024)

**Table 5** The Mamba-based methods in image-level vision tasks (Part II)

Methods	Block	Data	Task	Scan	Continuity	Code
<b>Object Detection</b>						
FER-YOLO-Mamba (Ma et al, 2024a)	VSS*	Facial Images	Facial Expression DET	BD (H/V/LD/RD)	Raster	✓
VMambaCC (Ma et al, 2024c)	VSS	Natural Images	Crowd Counting	BD (H/V)	Raster	
SOAR (Verma et al, 2024)	Vim	Remote Sensing Images	Small Object DET	BD (H)	Raster	✓
<b>Image Generation</b>						
DiS (Fei et al, 2024)	Vim	Natural Images	Image Generation	BD (H)	Raster	✓
ZigMa (Hu et al, 2024)	Mamba*	Natural Images	Image Generation	BD (H/V)	Zigzag	✓
DIM (Teng et al, 2024)	Mamba	Natural Images	Image Generation	BD (H/V)	Raster	✓
DIM <sup>†</sup> (Mo and Tian, 2024)	Mamba	Natural Images	Image Generation	BD (H)	Raster	
Gamba (Shen et al, 2024)	Mamba*	Natural Images	3D Reconstruction	SD (H)	Raster	
MD-Dose (Fu et al, 2024b)	Mamba	2D Medical Images (CT)	Radiation Dose Prediction	SD (H)	Raster	✓
VM-DDPM (Ju and Zhou, 2024)	VSS*	2D Medical Images (CXR/MRI)	2D Medical Image Synthesis	BD (H/V)	Raster	
SMCD (Qian et al, 2024)	Mamba*	Motion Sequence (Style/Content)	Motion Style Transfer	SD (H)	Raster	
<b>Image Restoration</b>						
UVMNet (Zheng and Wu, 2024)	Mamba*	Natural Images	Dehazing/Low Light Enhancement/Draining	SD (H) + Channel	Raster	✓
CU-Mamba (Deng and Gu, 2024)	Mamba*	Natural Images	Denosing/Deblurring	SD (H) + Channel	Raster	
ALGNet (Gao and Dang, 2024)	Mamba	Natural Images	Deblurring	SD (H)	Raster	
EVSSM (Kong et al, 2024)	VSS*	Natural Images	Deblurring	BD (H/V)	Raster	✓
FreqMamba (Zhen et al, 2024)	VSS*	Natural Images	Deraining	BD (H/V) + FT + Local Sampling	Raster	
DFSSM (Yamashita and Ikehara, 2024)	VSS*	Natural Images	Deraining	BD (H/V)	Raster	
FourierMamba (Li et al, 2024a)	VSS*	Natural Images	Deraining	BD (H/V) + FT	Raster	
MambaIR (Guo et al, 2024a)	VSS*	Natural Images	Super-resolution/Denoising	BD (H/V)	Raster	✓
VmambaIR (Shi et al, 2024b)	Mamba*	Natural Images	Super-resolution/Draining	BD (H/V/D)	Raster	✓
MMA (Cheng et al, 2024)	Vim*	Natural Images	Super-resolution	BD (H)	Raster	
DVMSR (Lei et al, 2024)	Mamba	Natural Images	Super-resolution	SD (H)	Raster	✓
IRSRMamba (Huang et al, 2024g)	VSS*	Natural Images	Super-resolution	BD (H/V)	Raster	✓
MambaUIE (Chen and Ge, 2024)	VSS*	Natural Images	Underwater Image Enhancement	BD (H/V)	Raster	✓
WaterMamba (Guan et al, 2024)	VSS*	Natural Images	Underwater Image Enhancement	BD (H/V) + Channel	Raster	
Retinexmamba (Bai et al, 2024)	VSS*	Natural Images	Low Light Enhancement	BD (H/V)	Raster	✓
FDVMNet (Zheng and Zhang, 2024)	Mamba*	2D Medical Images (Endo)	Endoscopic Exposure Correction	SD (H)	Raster	✓
MambaMIR (Huang et al, 2024b,c)	VSS*	3D Medical Images (FMRI/SVCT)	Medical Image Reconstruction	BD (H/V)	Raster	✓
MSDR (Li et al, 2024i)	VSS*	2D Medical Images (ODT)	Sparse Reconstruction	BD (H/V)	Raster	
HSIDMamba (Liu et al, 2024h)	VSS*/Vim*	Remote Sensing Images	Hyperspectral Denoising	BD (H/V/H*/V*)	Zigzag	
SSUMamba (Fu et al, 2024a)	Vim*	Remote Sensing Images	Hyperspectral Denoising	BD (H/V/D)	Raster	✓
RSDehamba (Zhou et al, 2024a)	VSS*	Remote Sensing Images	Dehazing	BD (H/V)	Raster	
FMSR (Xiao et al, 2024)	VSS*	Remote Sensing Images	Super-resolution	BD (H/V)	Raster	
GMSR (Wang et al, 2024e)	VSS*	Remote Sensing Images	Spectral Reconstruction	BD (H/V)	Raster	✓
<b>Others</b>						
MambaAD (He et al, 2024a)	VSS*	Natural Images	Multi-class Anomaly DET	BD (H/V/H*/V*)	Hilbert	✓
MambaVC (Qin et al, 2024)	VSS	Natural Images	Visual Compression	BD (H/V)	Raster	✓

is the first to leverage an SSM-CNN hybrid architecture in diffusion models for medical image synthesis. SMCD (Qian et al, 2024) is the first style motion conditional diffusion framework that treats style motion as a condition. It is also the first to apply Mamba to predict stylized motion in each sampling step.

#### 4.1.5 Restoration

Recently, the Mamba architecture has also been extensively applied to various image restoration tasks. These low-level tasks include reconstructing degraded images to their original state, such as image dehazing (Zheng and Wu, 2024), deraining (Zheng and Wu, 2024; Zhen et al, 2024), and super-resolution (Guo et al, 2024a; Cheng et al, 2024; Lei et al, 2024), and enhancing the image quality by adjusting luminance, contrast, and other visual attributes, such as low light enhancement (Zheng and Wu, 2024; Bai et al, 2024), and underwater image enhancement (Chen and Ge, 2024).

The extraction of local fine-grained features plays a critical role in tackling low-level image tasks such as dehazing, which the vanilla Mamba architecture lacks. Incorporating convolutions can enhance the visual representation of Mamba-based methods (Zheng and Wu, 2024). Additionally, the correlation between channels

is vital. UVMNet (Zheng and Wu, 2024) and CU-Mamba (Deng and Gu, 2024) processed the feature maps in both spatial and channel domains, in parallel and serially respectively. In image deblurring tasks, ALGNet (Gao and Dang, 2024) utilized simplified channel attention to model local connectivity. EVSSM (Kong et al, 2024) applied various geometric transformations before each SSM-based module instead of the common practice of scanning in four directions for efficient computation. It also introduced a frequency-domain-based Feedforward network. Image restoration approaches often utilize techniques from the frequency domain, leveraging the ability to isolate and manipulate specific image frequency components for improving detail recovery. For instance, high-frequency rain streaks in draining tasks are removed using frequency techniques (Zhen et al, 2024). Additionally, DFSSM (Yamashita and Ikehara, 2024) incorporated a mixed-scale gated convolutional block, and FourierMamba (Li et al, 2024a) employed a zigzag scanning strategy specifically designed for the frequency domain. Similarly, in image super-resolution tasks, techniques such as convolutions (Guo et al, 2024a; Lei et al, 2024), channel attention (Guo et al, 2024a; Cheng et al, 2024), channel scanning (Shi et al, 2024b), and frequency analysis (Huang et al, 2024g) are applied. Additionally, DVMSR (Lei



et al, 2024) employed a distillation strategy to enhance both efficiency and performance. In image enhancement tasks, MambaUIE (Chen and Ge, 2024) and WaterMamba (Guan et al, 2024) were specifically developed to improve the visual quality of underwater images degraded due to light absorption and scattering, integrating convolutions and spatial-channel scanning associate with multi-scale Feedforward network respectively. Retinexmamba (Bai et al, 2024) incorporated illumination-fused attention and the Mamba architecture for low light enhancement.

In the medical domain, FDVMNet (Zheng and Zhang, 2024) introduced a C-SSM block by combining convolution, SSM, cross-attention, and shortcut as a basic cell, and utilized two paths to process the phase and amplitude of the frequency domain information respectively. MambaMIR (Huang et al, 2024b,c) introduced an Arbitrary-Masked State Space (AMSS) block based on VSS by adopting an arbitrary-mask mechanism to leverage the scanning redundancy. MS DR (Li et al, 2024i) combined the VSS block and an Inception-based FeedForward Network module.

In the remote sensing domain, denoising and dehazing methods include zigzag scanning in eight spatial directions (Liu et al, 2024h), Spatial-Spectral Alternating Zigzag Scan strategy (Fu et al, 2024a), and Direction-aware Scan Module (Zhou et al, 2024a). Additionally, spectral attention (Liu et al, 2024h) and channel attention (Zhou et al, 2024a) were employed. FMSR (Xiao et al, 2024) was developed to improve spatial-frequency fusion in remote sensing image super-resolution tasks. GMSR (Wang et al, 2024e) introduced a gradient-guided Mamba for spectral reconstruction from RGB images.

#### 4.1.6 Others

Some works employ Mamba for other vision tasks. MambaAD (He et al, 2024a) applied Mamba to multi-class unsupervised anomaly detection. MambaVC (Qin et al, 2024) explored the use of Mamba architecture for visual compression.

## 4.2 Video

Video processing is one of the fundamental directions in computer vision. The primary goal of video processing is to effectively master spatio-temporal representations across long contexts. Mamba excels in this domain with its selective state space model, which achieves a balance between maintaining linear complexity and enabling effective long-term dynamic modeling. This innovative approach has been widely adopted in diverse

video analysis tasks such as video understanding (Li et al, 2024c) and video generation (Hu et al, 2024).

### 4.2.1 Video Understanding

Mamba-ND (Li et al, 2024d) extended the Selective State Model to higher dimensions, unraveling the input data across various dimensions in row-major order. In addition to the 2D image tasks previously discussed, it also explored mamba’s effectiveness in video action recognition tasks. VideoMamba (Li et al, 2024c) extended Vim’s original 2D scan into different bidirectional 3D spatiotemporal scans to build a purely SSM-based model for video understanding. It showcased the scalability of the Mamba backbone in the visual domain through the use of self-distillation pretraining techniques. VideoMamba set new benchmarks for video understanding across short-term, long-term, and multi-modal video tasks, providing a scalable and efficient solution for comprehensive analysis of video content. Different from VideoMamba, VideoMamba Suite (Chen et al, 2024a) did not introduce a novel method but rather focused on assessing whether Mamba can serve as a viable alternative to Transformers in the video understanding domain. It leveraged Mamba in four distinct roles: temporal models, temporal modules, multi-modal interaction models, and space-time sequence models to reveal Mamba’s effectiveness in video understanding and to emphasize its key characteristics. VideoMamba Suite demonstrated Mamba’s ability to efficiently handle complex spatial-temporal dynamics, showcasing both superior performance and favorable efficiency-performance trade-offs. RhythmMamba (Zou et al, 2024a) designed multi-temporal Mamba as well as frequency domain feed-forward channel interacting to enable Mamba to capture the quasi-periodic patterns of remote photoplethysmography (rPPG). This study also explored the performance of RhythmMamba under long-time series inputs, demonstrating its robust performance over arbitrary length videos. Simba (Chaudhuri and Bhattacharya, 2024) leveraged Mamba within a novel encoder-decoder architecture with a Shift-GCN backbone to address the challenge of efficiently modeling long sequences inherent in skeleton action recognition tasks. In (Chen et al, 2024b), the authors curated the first AI-generated video detection dataset, GenVideo, and introduced the DeMamba module to enhance detectors for this task. MAMBA4D (Liu et al, 2024b), the first Mamba-based 4D backbone, was developed for generic point cloud video understanding.

Vivim (Yang et al, 2024e) introduced a Mamba-based framework for medical video object segmenta-

**Table 6** The Mamba-based methods in video-level vision tasks. The abbreviations of Block here are VSS: Vision State Space Module, Vim: Vision Mamba, \*: modification. The abbreviations of Task here are CLS: Classification, SEG: Segmentation

Methods	Block	Data	Task	Code
<b>Video Understanding</b>				
Vivim (Yang et al, 2024e)	Vim*	Ultrasound Videos, Endoscopic Videos	Video Object SEG	✓
VideoMamba (Li et al, 2024c)	Vim*	Natural Videos	Action CLS, Long-form Video Understanding, Text-to-Video Retrieval	✓
VideoMamba Suite (Chen et al, 2024a)	Vim*	Natural Videos	Action Localization, Action anticipation, Action Recognition, Video Captioning Video Grounding, Video Question Answering, Multi-instance Retrieval	✓
RhythmMamba (Zou et al, 2024a)	Mamba*	Facial Videos	rPPG Prediction	✓
Simba (Chaudhuri and Bhattacharya, 2024)	Mamba	Skeletal Action Videos	Skeletal Action Recognition	✓
DeMamba (Chen et al, 2024b)	Mamba	Natural Videos	AI-Generated Video Detection	✓
MAMBA4D (Liu et al, 2024b)	Mamba	Point Cloud Videos	3D Action Recognition, 4D Semantic SEG	
<b>Video Generation</b>				
SSMDiff (Oshima et al, 2024)	Vim	Natural Videos	Video Generation	✓
ZigMa (Hu et al, 2024)	Mamba*	Natural Videos	Video Generation	✓
Matten (Gao et al, 2024)	Vim*	Natural Videos	Video Generation	
DiM <sup>†</sup> (Mo and Tian, 2024)	Mamba	Natural Videos	Video Generation	

**Table 7** The Mamba-based methods in point cloud vision tasks. The abbreviations of Block here are VSS: Vision State Space Module, Vim: Vision Mamba, \*: modification. The abbreviations of Task here are CLS: Classification, DET: Detection, SEG: Segmentation

Methods	Block	Data	Task	Code
PointMamba (Liang et al, 2024)	VSS*	3D Point Cloud Data	Object CLS, Part SEG	✓
PCM (Zhang et al, 2024d)	Vim*	3D Point Cloud Data	Object CLS, Part SEG, Semantic SEG	✓
PointMamba <sup>†</sup> (Liu et al, 2024d)	Vim*	3D Point Cloud Data	Object CLS, Semantic SEG	✓
Mamba3D (Han et al, 2024)	Vim*	3D Point Cloud Data	Object CLS, Part SEG	✓
PoinTramba (Wang et al, 2024h)	VSS	3D Point Cloud Data	Object CLS, Part SEG	✓
LCM (Zha et al, 2024)	Mamba	3D Point Cloud Data	Object CLS, Object DET, Part SEG	
3DMambaIPF (Zhou et al, 2024b)	Mamba	3D Point Cloud Data	Point Cloud Filtering	
3DMambaC (Li et al, 2024g)	Mamba*	3D Point Cloud Data	Point Cloud Completion	
EventMamba (Ren et al, 2024a)	Mamba*	3D Event Cloud Data	Action Recognition, Camera Pose Relocalization, Eye-tracking Regression	
OverlapMamba (Xiang et al, 2024)	Vim*	LiDAR Data	Place Recognition	✓

tion, featuring a novel temporal mamba block with spatiotemporal selective scanning.

#### 4.2.2 Video Generation

SSMDiff (Oshima et al, 2024) replaced the attention layers in diffusion models with bidirectional SSMs to facilitate the generation of long video sequences. Zigma (Hu et al, 2024) developed several spatially continuous, space-filling 2D scanning schemes for image generation. Additionally, it factorized the 3D Mamba model into 2D and 1D Zigzag Mamba to enhance the integration of spatial and temporal information in video generation. Matten (Gao et al, 2024) investigated a latent diffusion model for video generation. It explored four model variants with different combinations of Mamba and attention mechanisms, revealing that integrating attention mechanisms for capturing local spatiotemporal details, and Mamba architectures for capturing global information, yields optimal performance.

### 4.3 Point Cloud

Point cloud is a fundamental 3D representation, which provides continuous spatial position information with

3D coordinates. The intrinsic disorder and irregularity natures of point cloud have been a challenge in 3D vision. Inspired by the linear complexity and global modeling capabilities of Mamba, several general SSM-based backbones (Liang et al, 2024; Zhang et al, 2024d; Liu et al, 2024d; Zhou et al, 2024b; Li et al, 2024g; Han et al, 2024) have been investigated in the field of point cloud processing.

In common tasks such as classification and segmentation, some methods primarily explore logical geometric scanning orders to convert point clouds into 1D point sequences. These methods include reordering strategy (Liang et al, 2024), consistent traverse serialization (Zhang et al, 2024d), and octree-based ordering mechanism (Liu et al, 2024d). Mamba3D (Han et al, 2024) employed a bidirectional SSM with channel flipping, and introduced Local Norm Pooling (LNP) block to extract local geometric features. PoinTramba (Wang et al, 2024h) is a hybrid Transformer-Mamba framework and introduced a bi-directional importance-aware ordering strategy. LCM (Zha et al, 2024) applied the Mamba architecture to Masked Point Modeling (MPM) pre-training, and proposed a locally constrained compact point cloud model.

In addition, 3DMambaIPF (Zhou et al, 2024b) was developed for iterative filtering to remove the noise from the point cloud. 3DMambaC (Li et al, 2024g) was designed to transform an initially incomplete and low-quality point cloud into a complete and high-fidelity version. EventMamba (Ren et al, 2024a) introduced a Mamba-based point cloud framework for event camera classification and regression tasks. OverlapMamba (Xiang et al, 2024) first transforms input range views into feature sequences and then processes these sequences using bidirectional Mamba for place recognition.

#### 4.4 Multi-modal

Multi-modal tasks have become increasingly pivotal in the domain of computer vision, enabling the enrichment of visual understanding through the integration of diverse information sources. The fundamental objective of multi-modal tasks is to learn valuable potential feature representations from a multitude of modalities, such as textual captions and visual images, RGB images with supplementary components like depth or thermal images, and various forms of medical imaging data. Nevertheless, a significant challenge in attaining multi-modal objectives lies in the effective capture and amalgamation of the information across diverse modalities. Recently, several methods employ Mamba architecture for numerous multi-modal tasks, demonstrating impressive performance in comparison to approaches based on CNN and Transformer. According to the modal correlation of the input data, these methods can be categorized into two distinct paradigms: homogeneous multi-modal methods (§ 4.4.1) and heterogeneous multi-modal methods (§ 4.4.2).

##### 4.4.1 Homogeneous Multi-modal

Homogeneous multi-modal paradigm refers to the tasks where the input data consists of multiple modalities sharing similar data type, including MRI-CT registration (Guo et al, 2024b; Wang et al, 2024i), medical image fusion (Li et al, 2024h; Xie et al, 2024b), medical image generation (Atli et al, 2024), remote sensing images pansharpening (Cao et al, 2024; He et al, 2024b; Peng et al, 2024), infrared-visible image fusion (Li et al, 2024h; Ma et al, 2024b; Xie et al, 2024b), RGB-infrared image object detection (Li et al, 2024b; Dong et al, 2024; Li et al, 2024h) and RGB-thermal/depth image semantic segmentation (Wan et al, 2024).

For the infrared-visible image fusion tasks in the natural domain, several methods (Li et al, 2024h; Ma et al, 2024b; Xie et al, 2024b) employed Mamba

block to extract and integrate feature representations of RGB images and infrared images. Specifically, MambaDFuse (Li et al, 2024h) proposed a Mamba-based Dual-phase Fusion model, including dual-level single-modal feature extraction, dual-phase multi-modal feature fusion, and fused image reconstruction. FusionMamba<sup>†</sup> (Xie et al, 2024b) proposed a dynamic feature enhancement method based on Mamba, which integrates VSS block with dynamic convolution and channel attention. S4Fusion (Ma et al, 2024b) proposed the Saliency-aware Selective State Space Fusion model, which can simultaneously focus on global spatial information from both modalities while facilitating their interaction. Meanwhile, Fusion-Mamba (Dong et al, 2024), MambaDFuse (Li et al, 2024h) and CFMW (Li et al, 2024b) aimed to utilize cross-modality complementary information from RGB images and infrared images to effectively improve object detection performance. Fusion-Mamba (Dong et al, 2024) introduced a Fusion-Mamba block designed to map cross-modal features into a hidden state space for interaction, thereby reducing disparities between these features and enhancing the consistency of the fused representations. CFMW (Li et al, 2024b) introduced a new task of handling adverse weather conditions in visible-infrared object detection, and designed Cross-Modality Fusion Mamba modules to enhance multi-modal integration. Meanwhile, Sigma (Wan et al, 2024) introduced a Mamba network for multi-modal semantic segmentation, which includes a siamese feature extractor, a feature fusion module, and an upsampling decoder.

In the medical domain, MambaMorph (Guo et al, 2024b) and VMambaMorph (Wang et al, 2024i) focused on the MRI-CT registration task and respectively integrated Mamba block and Visual State Space (VSS) block into the U-shaped encoder-decoder architectures for efficient long-range correspondence modeling. I2I-Mamba (Atli et al, 2024) was designed to enhance multi-modal image generation tasks by integrating channel-mixed Mamba blocks within the bottleneck of a convolutional backbone. Meanwhile, both MambaDFuse (Li et al, 2024h) and FusionMamba<sup>†</sup> (Xie et al, 2024b) also focused on medical image fusion to learn structural and anatomical information from structural images such as CT and MRI and metabolic and functional information from functional images such as PET and SPECT.

For the remote sensing images pansharpening tasks in the remote sensing domain, PanMamba (He et al, 2024b) proposed channel swapping Mamba and cross-modal Mamba, designed for efficient information exchange and fusion between low-resolution multi-spectral and high-resolution panchromatic images. Fu-

**Table 8** The Mamba-based methods in Multi-modal Vision Tasks. The abbreviations of Block here are VSS: Vision State Space Module, Vim: Vision Mamba, \*: modification. The abbreviations of Data here are CT: Computed Tomography, PAN: Panchromatic Images, LRHS: Low-resolution Hyper-spectral Images, LRMS: Low-resolution Multi-spectral Images, MRI: Magnetic Resonance Imaging, PET: Positron Emission Tomography, SPECT: Single-photon Emission Computed Tomography. The abbreviations of Task here are CLS: Classification, DET: Detection, IVF: Infrared-visible Image Fusion, MIF: Medical Image Fusion, MCR: MRI-CT Registration, RSIP: Remote Sensing Images Pansharpening, SEG: Segmentation, SU: Scene Understanding, VQA: Visual Question Answering

Methods	Block	Data	Task	Code
<b>Homogeneous Multi-modal</b>				
MambaDFuse (Li et al, 2024h)	Mamba*	RGB Images & Infrared Images, MRI & CT/PET/SPECT	IVF, MIF, Object DET	
FusionMamba <sup>†</sup> (Xie et al, 2024b)	VSS*	RGB Images & Infrared Images, MRI & CT/PET/SPECT	IVF, MIF	✓
S4Fusion (Ma et al, 2024b)	VSS	RGB Images & Infrared Images	IVF	✓
Fusion-Mamba (Dong et al, 2024)	VSS*	RGB Images & Infrared Images	Object DET	
CFMW (Li et al, 2024b)	Mamba*	RGB Images & Infrared Images	Object DET	✓
Sigma (Wan et al, 2024)	VSS*	RGB Images & Thermal/Depth Images	Semantic SEG	✓
MambaMorph (Guo et al, 2024b)	Mamba	MRI & CT	MCR	✓
VMambaMorph (Wang et al, 2024i)	VSS	MRI & CT	MCR	✓
I2I-Mamba (Atli et al, 2024)	VSS*	Multi-Contrast MRI, MRI & CT	Image Generation	✓
PanMamba (He et al, 2024b)	VSS*	PAN & LRMS	RSIP	✓
FusionMamba (Peng et al, 2024)	VSS*	PAN & LRMS/LRHS, RGB & LRHS	RSIP	✓
LE-Mamba (Cao et al, 2024)	VSS*	PAN & LRMS/LRHS, RGB & LRHS	RSIP	
<b>Heterogeneous Multi-modal</b>				
InstructGIE (Meng et al, 2024)	VSS	Natural Images & Text	Image Editing	
VLmamba (Qiao et al, 2024)	VSS*	Natural Images & Text	VQA, Reasoning, SU	✓
Meteor (Lee et al, 2024)	Mamba	Natural Images & Text	VQA, Reasoning, SU	✓
Cobra (Zhao et al, 2024a)	Mamba	Natural Images & Text	VQA, Reasoning	✓
ReMamber (Yang et al, 2024d)	VSS*	Natural Images & Text	Referring Image SEG	
CLIP-Mamba (Huang et al, 2024f)	VSS/Mamba*	Natural Images & Text	Zero-shot CLS, Out of Distribution CLS	✓
SurvMamba (Chen et al, 2024g)	Vim*	Whole Slide Images & Gene	Survival Prediction	
RSCaMa (Liu et al, 2024a)	Vim*	Remote Sensing Images & Text	Change Captioning	✓
SpikeMba (Li et al, 2024e)	Vim*	Natural Videos & Text	Temporal Video Grounding	
BroadMamba (Shou et al, 2024)	Vim*	Audio & Video & Text	Emotion Recognition	
Coupled Mamba (Li et al, 2024f)	Mamba*	Audio & Video & Text	Sentiment Analysis	
Mamba-FETTrack (Huang et al, 2024a)	Vim*	Video & Event Data	Frame-event Tracking	✓
MotionMamba (Zhang et al, 2024e)	Mamba*	Motion Sequence & Text	Motion Generation	✓
TM-Mamba (Wang et al, 2024f)	Vim*	Motion Sequence & Text	Human Motion Grounding	

sionMamba (Peng et al, 2024) incorporated VSS blocks into two U-shaped networks for extracting spatial and spectral features, and proposed the FusionMamba block by expanding SSM to accommodate dual inputs. LE-Mamba (Cao et al, 2024) introduced the Local Enhancement Vision Mamba block, which partitions the input image into windows for processing, and a state sharing technique to enhance the interaction between spatial and spectral information.

#### 4.4.2 Heterogeneous Multi-modal

Heterogeneous multi-modal paradigm refers to the tasks where the input data consists of multiple modalities with different data types. In the field of text-driven generation, Mamba architectures are utilized for visual processing. To enhance the generalization capabilities of image editing approaches, InstructGIE (Meng et al, 2024) reformed the conditional latent diffusion model by integrating a vision encoder based on VMamba, and used the VMamba layer to inject the processed visual condition information into the frozen Stable Diffusion (Rombach et al, 2022) model. In the realm

of Multimodal large language models (MLLMs), VL-Mamba (Qiao et al, 2024) replaced the transformer-based backbone language model such as LLaMa (Touvron et al, 2023) with the pre-trained Mamba language model. Additionally, it introduced the Multi-Modal Connector, comprising a Vision Selective Scan (VSS) module and two linear layers. Meteor (Lee et al, 2024) introduced multifaceted rationales and applied the Mamba architecture to embed these lengthy rationales to enhance the understanding and answering capabilities of MLLMs. Cobra (Zhao et al, 2024a) introduced a linear computational complexity MLLM, utilizing DINOv2 (Oquab et al, 2023) and SigLIP (Zhai et al, 2023) as vision encoder and directly employing the Mamba language model as the backbone. ReMamber (Yang et al, 2024d) is a novel referring image segmentation framework containing several Mamba Twister blocks. Each block comprises Visual State Space (VSS) layers to extract the vision feature and a twister layer to integrate the textual information into the visual modality. CLIP-Mamba (Huang et al, 2024f) is the first to train a transferable Mamba model using Contrastive Language-Image Pre-training (CLIP).

It demonstrated that compared to ViT, Mamba is more parameter-efficient in zero-shot classification tasks and exhibits exceptional robustness in out-of-distribution (OOD) tasks. Additionally, Hessian visualizations suggest that Mamba models may face challenges in optimization. SurvMamba (Chen et al, 2024g) was designed to enhance the accuracy of survival prediction by integrating pathological images and genomic data. It introduced the Hierarchical Interaction Mamba (HIM) to facilitate efficient intra-modal interactions at different granularities, and the Interaction Fusion Mamba to aggregate the cascaded multi-modal features. RSCaMa (Liu et al, 2024a) employed multiple CaMa layers between the backbone and the language decoder to facilitate efficient joint spatial-temporal modeling for remote sensing image change captioning.

SpikeMba (Li et al, 2024e) combined the Mamba and Spiking mechanism for temporal video grounding. It comprises the Mamba-based Contextual Moment Reasoner with learnable relevant slots, Spiking Saliency Detector, and Multi-modal Relevant Mamba. BroadMamba (Shou et al, 2024) applied the Mamba architecture to multimodal emotion recognition in conversation, and designed a Broad Mamba using bidirectional SSM for the feature disentanglement stage, enabling the extraction of long-range contextual semantic information from different modalities. Coupled Mamba (Li et al, 2024f) proposed coupling state chains of inter-modalities while maintaining the independence of intra-modality state processes. It also derived the global convolution kernel to enable parallelism for the coupled state transition scheme.

Mamba-FETTrack (Huang et al, 2024a) introduced a RGB-Event tracking framework that integrates video frames and event streams for target object localization. The framework employed the Mamba architecture for modality-specific feature extraction and multi-modal feature fusion. Motion Mamba (Zhang et al, 2024e) incorporated two modules based on the vanilla Mamba into a diffusion-based generative system for text-to-motion synthesis, namely hierarchical temporal Mamba and bidirectional spatial Mamba. TM-Mamba (Wang et al, 2024f) introduced a novel text-based motion grounding task and employed the bidirectional SSM to construct the text-controlled selection mechanism, dynamically incorporating global temporal information from the motion sequence based on the text query.

## 5 Challenges and Future Directions

In this section, we identify current challenges and outline promising directions, to enhance Mamba’s capabilities and broaden its applications in computer vision.

### 5.1 Scalability

#### 5.1.1 Model Size

In the current era of large foundation models, the scalability of deep neural networks is pivotal for advancing general artificial intelligence. Mamba is emerging as a promising foundational architecture, offering an alternative to prevalent Transformers with its ability to scale linearly with sequence length. However, while existing techniques aimed at reducing the computational complexity of Transformers often compromise on model expressivity or adaptability, Mamba also encounters challenges when scaled to large-sized networks.

Firstly, the Mamba architecture faces stability issues when scaled to large network configurations (Patro and Agneeswaran, 2024a). The underlying causes of Mamba’s instability remain inadequately understood. This instability often manifests as vanishing or exploding gradients (Patro and Agneeswaran, 2024b), leading to performance degradation or even training collapse. To address the stability issues, some studies utilize stable reparameterization to balance gradient scales in state space models (Wang and Li, 2024). Some works utilize learnable Fourier Transforms to adjust the eigenvalues of the evolution matrix, ensuring they are negative real numbers, which helps maintain stability (Patro and Agneeswaran, 2024b). Despite these efforts, most visual Mamba models are limited to base or smaller scales, which may restrict their performance.

Secondly, visual Mamba models, when controlled for similar parameters or FLOPs, are generally outperformed by cutting-edge CNNs, advanced visual Transformers, and hybrid architectures that integrate multiple model types. This performance gap also hinders the scaling of visual Mamba models and underscores the necessity to enhance their performance. Integrating architectures or techniques proven effective in CNNs and visual Transformers could help bridge the performance gap. Besides, while there may be some compromise in performance, the non-hierarchical architectures comprising identical blocks facilitate optimization for hardware acceleration. This aspect is crucial for scaling to large models and enhancing computational efficiency. In addition, self-supervised pre-training plays a critical role in enhancing the model performance. For instance, ARM (Ren et al, 2024b) demonstrates that the autoregressive pre-training can significantly improve the performance of the Mamba architecture and address the instability issues, efficiently unlocking its potential for scaling to very large model sizes. However, the self-supervised pre-training strategies for Mamba models are still nascent.

Future research should focus on optimizing these aspects to harness the full capabilities of large network configurations.

### 5.1.2 Data

The Mamba architecture theoretically reduces computational complexity, which enhances its efficiency for processing long sequence data. Moreover, unlike many sequence models that do not benefit from extended contexts (Shi et al, 2023), Mamba can selectively disregard irrelevant information, resulting in consistent performance improvements as context length increases. The efficiency and efficacy of Mamba architecture bring significant opportunities for data scalability.

Firstly, the Mamba architecture offers significant potential for effectively handling high-dimensional data by treating each sample as a long sequence. This capability is particularly beneficial for processing high-resolution and multi-dimensional data including high-resolution remote sensing images, whole slice pathology images, hyperspectral and multispectral images, 3D medical images, and point clouds. Secondly, its efficiency and prowess in long sequence modeling not only facilitate scaling to large-scale datasets, but also enable effective analysis of the temporal or spatial relationships among samples. The typical datasets include multi-temporal remote sensing images, where changes over time provide essential information, and long-term video frames, where continuous activities must be analyzed over extended periods.

Furthermore, given the parameter efficiency of the Mamba models and their inherent local inductive bias, which typically mitigate overfitting, Mamba models have considerable potential for achieving optimal performance without relying on large-scale datasets. This opens up opportunities for developing small yet effective Mamba-based models advantageous in resource-constrained environments, a pathway that has not been extensively explored in current research.

Future research should concentrate on scaling Mamba models for processing visual data with higher dimensions and larger scales. Fully exploiting the visual data by designing small models that maintain high performance is also a promising future direction.

### 5.1.3 Hardware-aware

Previous SSMs such as S4 are time- and input-invariant, making it feasible to unroll the recurrent representation into the convolutional representation for efficient parallel computation during training. However, the selection mechanism in Mamba makes the model become time-

and input-dependent, making it infeasible to train the model under the convolutional representation. To overcome this limitation of the selective SSMs (Mamba) and make them efficient on modern hardware, hardware-aware algorithm has been designed to accelerate the training under the recurrent mode.

Mamba uses kernel fusion and recomputation to make the computation of the parallel SSM scan fast and memory-efficient. Specifically, the discretization step, the scan, and the multiplication with the projection matrix are fused into one kernel. Then the SSM parameters are loaded from slow HBM to fast SRAM for calculating the fused kernel in SRAM. Subsequently, the outputs are written back to HBM. In addition, Mamba chooses to recompute the intermediate states for the backpropagation since the recomputation is faster than storing them and reading them from HBM. These two strategies accelerate the scan operation and reduce the GPU requirement.

However, according to research findings (Wang et al, 2024g; Dao and Gu, 2024), GPU consumption for the Mamba model does not consistently demonstrate a reduction compared to the Transformer model, highlighting the need for optimized, hardware-aware Mamba algorithms tailored for vision tasks. Mamba-2 (Dao and Gu, 2024) establishes theoretical connections between structured SSMs and variants of attention by reformulating different approaches to computing SSMs as various matrix multiplication algorithms on structured matrices and generalizing the linear attention (Katharopoulos et al, 2020) to structured masked attention. Based on this theoretical analysis, Mamba-2 introduces an efficient State Space Duality (SSD) algorithm for SSM computation and modifies the Mamba block to be tensor parallelism friendly. This framework allows Mamba-2 to leverage system optimizations developed for Transformers, including tensor parallelism and sequence parallelism, facilitating the parallel training of large models using multiple GPUs. Moreover, unlike Transformers, Mamba-2 can be efficiently trained with variable sequence lengths. However, the adaptation of Mamba-2 to vision tasks remains an area that requires further investigation.

Future research should focus on developing hardware-aware approaches to enhance the computational efficiency of visual Mamba models. On the one hand, hardware-aware approaches that reduce computational overhead are essential for scaling to larger hardware configurations. On the other hand, from a broader perspective, they are crucial for the development of green artificial intelligence technologies, which attract more and more attention from the community due to

the need for energy consumption reduction to protect the environment.

#### 5.1.4 Task

The Mamba architecture, noted for its efficiency and proficiency in long sequence modeling, enables applications across a broader spectrum of tasks compared to CNNs and Transformers.

Firstly, as previously mentioned, the Mamba architecture offers broader possibilities for handling high-dimensional data and large-scale datasets.

Secondly, the Mamba model’s proficiency in handling extended sequences significantly enhances its applicability in multi-modal learning. Similar to the Transformer, which effectively models both natural languages and images within a unified framework, the long sequence modeling capability of the Mamba architecture allows it to involve more modalities such as time series and extended textual content. Besides, like the Transformer, Mamba can adeptly handle concatenated independent sequences, processing them either as a whole or as distinct entities by resetting their states at boundaries. Furthermore, Mamba offers computational efficiency and time-scale robustness, the latter of which is particularly advantageous for addressing issues with missing modalities in data streams.

Thirdly, the high efficiency of the Mamba architecture enables the development of high-speed and highly efficient applications. This includes interactive systems, autonomous driving, and surveillance, where real-time processing and reduced computational overhead are critical.

Future research should focus on effectively leveraging the Mamba architecture to enhance performance in existing tasks and to explore new applications.

## 5.2 Causality

In visual Transformer-based architectures, the attention matrix explicitly captures dependencies between each pair of visual tokens, enabling predictions at any location to have a global receptive field. However, in Mamba-based architectures, the S6 blocks make predictions for each token based solely on the hidden state  $h_{t-1}$  and the current input  $x_t$ . The  $h_{t-1}$  only incorporates information from previously scanned tokens and disregards information from other tokens. Consequently, the vanilla Mamba is a causal system where predictions rely solely on the current and previous inputs. Although the causality is naturally suitable for autoregressive models in sequential vision tasks (Ren et al, 2024b), it contradicts the nature of spatial images,

resulting in a fundamental mismatch between Mamba-based architectures and common visual tasks. To address this issue, existing works have proposed to integrate multiple scanning directions to ensure a global receptive field. While these strategies partially mitigate the undesirable causality of Mamba in vision tasks, they still encounter challenges or introduce new drawbacks that require resolution.

Firstly, while the utilization of multiple scanning directions helps establish a global receptive field, this approach does not effectively address the underlying causality issue. Tokens at different locations are still treated inconsistently due to their varying positions within the sequences, inevitably leading to a prioritization of more recently scanned tokens. Consequently, this strategy struggles to preserve spatial relationships and inadvertently introduces undesired bias for vision recognition as a result of the scanning order. In contrast, the self-attention mechanism in Transformers consistently consider all tokens to capture dependencies, showcasing its superiority to Mamba.

Secondly, the incorporation of multiple scanning strategies leads to redundancy and sub-optimal performance. To enhance Mamba’s perception at different locations, numerous approaches incorporate not only different scanning directions but also different scanning modes, axes, and continuity. While incorporating more scanning strategies may increase the information captured in specific locations, it introduces a significant amount of redundant information within these scanning sequences. This redundancy can impact model efficiency and hinder effective knowledge extraction for vision tasks.

Consequently, designing an appropriate approach for Mamba to consistently and elegantly consider tokens at different locations remains a critical challenge in visual data processing.

## 5.3 In-context Learning

Transformer models exhibit in-context learning (ICL) capabilities after large-scale pre-training, enabling them to learn new tasks with a few demonstrations without further explicit training or fine-tuning. In the dynamic landscape of deep learning, ICL methodologies have evolved to address increasingly complex tasks across NLP, CV, and multi-modal domains. These methodological advancements are pivotal for pushing the limits of existing deep learning frameworks.

Currently, Transformer models are the primary large models possessing ICL capabilities. The efficiency and long sequence modeling ability of Mamba make it a



promising alternative to Transformers for ICL. Furthermore, the inherent causality of the Mamba model eliminates the need for position embeddings, which are typically a constraint in extending the ICL capabilities of Transformers. In (Park et al, 2024), the authors investigate the ICL capabilities of Mamba compared to Transformers, focusing on regression ICL tasks and small-scale models. The results demonstrate that Mamba is capable of ICL and performs comparably to Transformers in standard regression ICL tasks. Additionally, Mamba outperforms Transformers in tasks such as sparse parity learning. However, Mamba struggles with tasks involving non-standard retrieval functionality, which Transformers can handle with ease. Research detailed in (Grazzi et al, 2024) further demonstrates Mamba’s capabilities on more complex NLP in-context tasks and shows that Mamba’s ICL efficacy scales positively with the number of in-context examples.

With its proficient in-context modeling capabilities and adeptness at capturing long-range dependencies, the Mamba model shows promising potential for deeper semantic understanding and enhanced performance in ICL applications.

## 5.4 Trustworthiness

### 5.4.1 Interpretability

Some studies have provided experimental evidence to elucidate the mechanisms underlying the Mamba model in NLP, focusing on its in-context learning capabilities (Grazzi et al, 2024; Park et al, 2024) and factual recall capabilities (Sharma et al, 2024). Additionally, other works (Cirone et al, 2024) have laid theoretical foundations for Mamba’s applications in NLP. Despite these advancements, explaining why Mamba performs effectively on visual tasks remains challenging. In (Ali et al, 2024), the authors reinterpret Mamba layers as self-attention mechanisms, thereby shedding light on its functionality both empirically and theoretically. However, the distinct learning characteristics of visual Mamba and its parallels with other foundational architectures, such as RNNs, CNNs, and ViTs, still demand deeper interpretation.

### 5.4.2 Generalization

According to findings in (Long et al, 2024), the hidden states in Mamba are likely to accumulate or even amplify domain-specific information, which can adversely affect its generalization performance. Moreover, the 1D scanning strategies inherent to the model may inadvertently capture domain-specific biases, and cur-

rent scanning techniques often fail to address the need for domain-agnostic information processing. Addressing these challenges to better harness Mamba’s strengths while improving its generalization remains a critical area for future research.

### 5.4.3 Safety

Research presented in (Du et al, 2024) demonstrates VMamba’s (Liu et al, 2024g) strengths in adversarial resilience and general robustness. However, it also identifies limitations in scalability when dealing with these tasks. The study includes white-box attacks on VMamba to examine the behavior of its novel components under adversarial conditions. The findings indicate that while parameter  $\Delta$  exhibits robustness, parameters  $\mathbf{B}$  and  $\mathbf{C}$  are susceptible to attacks. This differential vulnerability among parameters contributes to VMamba’s scalability challenges in maintaining robustness. Furthermore, the results reveal that VMamba exhibits particular sensitivity to interruptions in the continuity of its scanning trajectory and the integrity of spatial information. Enhancing the safety of visual Mamba remains an unresolved challenge in the field.

## 6 Conclusion

Mamba has rapidly emerged as a transformative long sequence modeling architecture, renowned for its exceptional performance and efficient computational implementation. As it continues to gain significant attraction in the field of computer vision, this paper offers a comprehensive review of visual Mamba approaches. We begin with an in-depth overview of the Mamba architecture, progressing to detailed examinations of representative visual Mamba backbone networks and their extensive applications. These applications are systematically categorized by differing modalities, including image, video, point cloud, and multi-modal data. Finally, we analyze the challenges and delineate future directions for visual Mamba, providing valuable outlooks that may influence ongoing and future developments in this dynamically evolving field.

## Declarations

*Funding:* This work was supported by the Hong Kong Innovation and Technology Fund (Project No. MHP/002/22), Project of Hetao Shenzhen-Hong Kong Science and Technology Innovation Cooperation Zone (HZQB-KCZYB-2020083) and the Research Grants Council of the Hong Kong (Project Reference Number: T45-401/22-N).

## A Visual Mamba Backbone Networks

In this section, we detail representative visual Mamba backbone networks that are briefly introduced in the main body of our paper.

Mamba (Gu and Dao, 2023), Vim (Zhu et al, 2024a), and VMamba (Liu et al, 2024g) are three critical architectures. All pure Mamba and hybrid Mamba networks can be regarded as variants of these architectures. They are frequently utilized or modified for diverse vision applications. Therefore, we compare their block algorithms to clarify their differences and enhance the understanding of each. The algorithmic details of the Mamba, Vim, and VSS blocks are presented in Algorithm 1, Algorithm 2, and Algorithm 3, respectively. As seen, Mamba and Vim perform scanning to transform 2D images into 1D sequences and apply multiplication after each selective State Space Model (SSM) operation. In contrast, VMamba extends the 1D SSM operations to 2D via scanning and applies multiplication after 2D SSM operation.

### A.1 Pure Mamba

*Mamba-ND*: Mamba-ND (Li et al, 2024d) aims to extend Mamba to multi-dimensional data including images and videos. It treats 1D Mamba layer as a black box and explores how to unravel and order the multi-dimensional data. It mainly addresses the challenges presented by data lacking a predefined ordering while possessing inherent spatial dimensions. Given the large quantities of possible ways of flattening the data into 1D sequence, Mamba-ND only includes the scan ordering by flattening the data along its dimension axes in the forward or backward direction. Then it applies the Mamba-ND block, which is a combination of 1D Mamba layers, to the sequence in alternating orderings. The authors conduct extensive experiments to explore different combinations of orderings. In addition, they split the input data’s one dimension into the number of orderings, adopt different arrangements of Mamba layers, and factorize the sequence into smaller sequences. Results show that a chain of Mamba layers and simple alternating-directional orderings achieve superior performance.

*FractalMamba*: To overcome the limitations in capturing spatial relationships inherent to linear scanning curves for image patches, FractalMamba (Tang et al, 2024b) adopts a fractal scanning curve, namely the Hilbert curve, for processing 2D image patches. The Hilbert curve method involves systematically halving and alternating the horizontal and vertical dimensions of the image at each recursion, according to the relevant quadrant. This structured traversal strategy ensures that image patches adjacent on the curve also remain proximate within the image’s two-dimensional spatial configuration. To further mitigate disruptions in local continuity, FractalMamba implements a simple yet effective shift operation, which adjusts the position of the curves up or down by one pixel. The FractalMamba block integrates four Hilbert curves oriented in four different directions into the Mamba block, enhancing the SSM’s ability to capture diverse spatial relationships.

*Mamba<sup>®</sup>*: Mamba<sup>®</sup> (Wang et al, 2024a) identifies that the feature artifacts observed in vision Transformers are more pronounced in Vim (Zhu et al, 2024a). These artifacts

manifest as anomalously high normalization values in low-information background regions, contrary to the expectation that informative foreground regions should exhibit high normalization values (Darcet et al, 2024).

To alleviate this issue, Mamba<sup>®</sup> refines Vim (Zhu et al, 2024a) by strategically inserting input-independent tokens, referred to as register (Darcet et al, 2024) tokens, into the visual token sequence. These register tokens are recycled and concatenated to form a comprehensive representation during final prediction. Through these modifications, Mamba<sup>®</sup> not only produces qualitatively cleaner and more semantically meaningful feature maps but also demonstrates quantitatively stronger performance and enhanced scalability. Furthermore, even without explicit optimization, different registers display distinct patterns that, in certain cases, effectively highlight various objects or semantic elements.

*ARM*: ARM (Ren et al, 2024b) identifies that the Mamba architecture, which enforces each token to attend only to its preceding tokens, aligns well with the principles of autoregressive modeling. Autoregressive pre-training of Mamba brings performance improvement and higher overall training efficiency. More importantly, it successfully enables Mamba to scale to large and even huge model configurations.

Autoregressive modeling involves defining the prediction units and sequentially modeling each unit based on all preceding units. To implement autoregressive modeling, ARM first converts the input image into patch tokens as the autoregressive inputs. Subsequently, to integrate 2D spatial information, it aggregates spatially adjacent patches into larger clusters as the prediction units. These clusters are sequenced in a row-first and forward order based on the empirical findings. With regards to the architecture, ARM stacks multiple MambaMLP blocks, which employ Mamba for sequence modeling and the multi-layer perceptron (MLP) for channel modeling. During pre-training, the Mamba layer within the MambaMLP block uses unidirectional scanning to match the autoregressive modeling. During fine-tuning, the Mamba layer scans the clusters in four directions, similar to the technique in VMamba (Liu et al, 2024g).

### A.2 Hybrid Mamba

*MSVMamba*: To balance performance with efficiency, MSVMamba (Shi et al, 2024a) modifies the SS2D scanning used in VMamba (Liu et al, 2024g) by downsampling the image in three directions within SS2D to shorten the sequence length, forming a Multi-Scale 2D (MS2D) scanning strategy. The MS2D decreases computational complexity and information redundancy, and introduces an additional hierarchical design within the block of the already hierarchical VMamba (Liu et al, 2024g) architecture. Additionally, each MSVMamba block incorporates a Convolutional Feed-Forward Network (ConvFFN) to enhance channel-wise information exchange and local feature extraction.

*SiMBA*: SiMBA (Patro and Agneeswaran, 2024b) aims to address the instability issue of Mamba scaling to large networks on vision datasets. It uses Mamba for sequence modeling and proposes a new channel modeling technique termed Einstein FFT (EinFFT). The EinFFT applies the Fourier Transform and performs Einstein Matrix Multiplication (EMM) in the frequency domain. Specifically, EMM

**Algorithm 1** Mamba Block Process

---

**Input:** token sequence  $X_{l-1} : (B, M, D)$   
**Output:** token sequence  $X_l : (B, M, D)$   
 # normalize the instance sequence  $X_{l-1}$   
 $X'_{l-1} : (B, M, D) \leftarrow \text{LayerNorm}(X_{l-1})$      $x : (B, M, E) \leftarrow \text{Linear}^x(X'_{l-1})$      $z : (B, M, E) \leftarrow \text{Linear}^z(X'_{l-1})$   
 # process sequences with single direction  
 $x' : (B, M, E) \leftarrow \text{SiLU}(\text{Conv1d}(x))$      $B_o : (B, M, N) \leftarrow \text{Linear}^B(x')$      $C_o : (B, M, N) \leftarrow \text{Linear}^C(x')$   
 # softplus ensures positive  $\Delta$   
 $\Delta : (B, M, E) \leftarrow \log(1 + \exp(\text{Linear}^A(x') + \text{Parameter}^A))$   
 $\bar{A} : (B, M, E, N) \leftarrow \Delta_o \otimes \text{Parameter}^A_o$      $\bar{B} : (B, M, E, N) \leftarrow \Delta_o \otimes B$   
 $y : (B, M, E) \leftarrow \text{SSM}(\bar{A}, \bar{B}, C)(x)$   
 # get gated  $y$   
 $y' : (B, M, E) \leftarrow y \odot \text{SiLU}(z)$   
 # residual connection  
 $X_l : (B, M, D) \leftarrow \text{Linear}(y') + X_{l-1}$   
**return**  $X_l$

---

**Algorithm 2** Vim Block Process

---

**Input:** token sequence  $X_{l-1} : (B, M, D)$   
**Output:** token sequence  $X_l : (B, M, D)$   
 # normalize the instance sequence  $X_{l-1}$   
 $X'_{l-1} : (B, M, D) \leftarrow \text{LayerNorm}(X_{l-1})$      $x : (B, M, E) \leftarrow \text{Linear}^x(X'_{l-1})$      $z : (B, M, E) \leftarrow \text{Linear}^z(X'_{l-1})$   
 # process sequences with distinct direction  
**for**  $o$  in {forward, backward} **do**  
    $x'_o : (B, M, E) \leftarrow \text{SiLU}(\text{Conv1d}_o(x))$      $B_o : (B, M, N) \leftarrow \text{Linear}^B_o(x'_o)$      $C_o : (B, M, N) \leftarrow \text{Linear}^C_o(x'_o)$   
   # softplus ensures positive  $\Delta_o$   
    $\Delta_o : (B, M, E) \leftarrow \log(1 + \exp(\text{Linear}^A_o(x'_o) + \text{Parameter}^A_o))$   
    $\bar{A}_o : (B, M, E, N) \leftarrow \Delta_o \otimes \text{Parameter}^A_o$      $\bar{B}_o : (B, M, E, N) \leftarrow \Delta_o \otimes B_o$   
    $y_o : (B, M, E) \leftarrow \text{SSM}(\bar{A}_o, \bar{B}_o, C_o)(x'_o)$   
**end for**  
 # get gated  $y_o$   
 $y'_{\text{forward}} : (B, M, E) \leftarrow y_{\text{forward}} \odot \text{SiLU}(z)$      $y'_{\text{backward}} : (B, M, E) \leftarrow y_{\text{backward}} \odot \text{SiLU}(z)$   
 # residual connection  
 $X_l : (B, M, D) \leftarrow \text{Linear}(y'_{\text{forward}} + y'_{\text{backward}}) + X_{l-1}$   
**return**  $X_l$

---

**Algorithm 3** VMamba Block Process

---

**Input:** feature map  $X_{l-1} : (B, H, W, D)$   
**Output:** feature map  $X_l : (B, H, W, D)$   
 # normalize the instance sequence  $X_{l-1}$   
 $X'_{l-1} : (B, H, W, D) \leftarrow \text{LayerNorm}(X_{l-1})$      $x : (B, H, W, E) \leftarrow \text{Linear}^x(X'_{l-1})$      $z : (B, H, W, E) \leftarrow \text{Linear}^z(X'_{l-1})$   
 # employ depth-wise convolutional layer for  $x$   
 $x' : (B, H, W, E) \leftarrow \text{SiLU}(\text{DWConv}(x))$   
 # process sequences with cross-scan  
**for**  $o$  in {HF, HB, VF, VB} **do**  
    $x'_o : (B, M, E) \leftarrow T_o(x')$      $B_o : (B, M, N) \leftarrow \text{Linear}^B_o(x'_o)$      $C_o : (B, M, N) \leftarrow \text{Linear}^C_o(x'_o)$   
   # softplus ensures positive  $\Delta_o$   
    $\Delta_o : (B, M, E) \leftarrow \log(1 + \exp(\text{Linear}^A_o(x'_o) + \text{Parameter}^A_o))$   
    $\bar{A}_o : (B, M, E, N) \leftarrow \Delta_o \otimes \text{Parameter}^A_o$      $\bar{B}_o : (B, M, E, N) \leftarrow \Delta_o \otimes B_o$   
    $y_o : (B, M, E) \leftarrow \text{SSM}(\bar{A}_o, \bar{B}_o, C_o)(x'_o)$   
**end for**  
 # get gated  $y_o$   
 $y' : (B, M, E) \leftarrow \sum_{o \in \{HF, HB, VF, VB\}} y_o$      $y' : (B, M, E) \leftarrow y' \odot \text{SiLU}(z)$   
 # residual connection  
 $X_l : (B, M, D) \leftarrow \text{Linear}(y') + X_{l-1}$   
**return**  $X_l$

---

reorganizes the input and the weight matrix along the channel dimensions into blocks, such that each block is a diagonal matrix for efficient computation. The EinFFT computes the real and imaginary parts of frequency components separately. EinFFT leverages Rayleigh’s Theorem, which posits that the energy of an image patch predominantly resides within a limited number of frequency components, and EinFFT is tailored to capture essential frequency patterns efficiently. Post-multiplication, a non-linear activation function is applied to modulate the eigenvalues in the Mamba block to ensure stability following the principle that stability is achieved if all eigenvalues of the evolution matrix are negative real numbers (Oppenheim and Verghese, 2010). The SiMBA block is comprised of a Mamba block and an EinFFT block, both interleaved with the LN layer, dropout, and residual connections.

**Vim-F:** Vim-F (Zhang et al, 2024b) identifies two main drawbacks of Vim (Zhu et al, 2024a). First, the image flattening method adopted by Vim disrupts the local dependencies and increases the distances between vertically adjacent tokens. Second, due to the patch embedding method implemented using non-overlapping convolutions and the bidirectional horizontal scanning strategy, Vim requires position embeddings to model the spatial relationships of tokens in the vertical direction.

To address the two identified drawbacks, Vim-F (Zhang et al, 2024b) utilizes the Fourier transform to transfer the feature map into the frequency domain and adds it to the original feature map. Since each point in the frequency feature map depends on the entire original feature map, frequency-domain scanning ensures a comprehensive global receptive field. Moreover, the translation invariance characteristic of the Fourier transform helps to mitigate the inductive bias introduced by the scanning strategy. Vim-F further eliminates the need for position embedding and introduces a new patch embedding method tailored for Mamba, employing overlapping convolutions to model the spatial correlation between tokens.

### A.3 Additional Results

In this section, we provide additional results of different visual Mamba backbone networks compared with popular architectures based on CNNs or Transformers on the object detection and instance segmentation benchmark. The performance is evaluated on the MS COCO (Lin et al, 2014) using Mask R-CNN (He et al, 2017) and the results from the respective papers are listed in Table. 9.

The object detection and instance segmentation performance aligns with the analysis in the main body of our paper. Specifically, all the models conform to the scaling law, and Mamba’s ability to capture long-range dependencies and employ dynamic weights proves advantageous for dense prediction tasks. However, Mamba-based models exhibit inferior performance compared to some Transformer-based approaches, which may be attributed to the selection mechanism. Additionally, existing Mamba-based models lack specific optimization for dense prediction tasks, highlighting opportunities for future research to explore and improve their effectiveness.

**Table 9** Results of object detection and instance segmentation on MS COCO (Lin et al, 2014) *mini-val* using Mask R-CNN (He et al, 2017) 3× schedule. FLOPs are computed using an input size 1280×800. † indicates FLOPs computed using an input size 1333×800. ‘MS’ denotes the utilization of multi-scale training. The **best**, **second-best**, and **third-best** results are bolded and distinguished using red, blue, and green, respectively

Backbone	Params	FLOPs	AP <sup>b</sup>	AP <sup>b</sup> <sub>50</sub>	AP <sup>b</sup> <sub>75</sub>	AP <sup>m</sup>	AP <sup>m</sup> <sub>50</sub>	AP <sup>m</sup> <sub>75</sub>
CNNs								
ConvNeXt-T (Liu et al, 2022b)	48.0 M	262.0 G	46.2	67.9	50.8	41.7	65.0	44.9
ConvNeXt-S (Liu et al, 2022b)	70.0 M	348.0 G	<b>47.9</b>	70.0	52.7	<b>42.9</b>	66.9	46.2
Transformers								
ViT-Adpt-S (Chen et al, 2023)	47.8 M	-	48.2	69.7	52.5	42.8	66.4	45.9
Swin-T (Liu et al, 2021)	48.0 M	267.0 G	46.0	68.1	50.3	41.6	65.1	44.9
Swin-S (Liu et al, 2021)	69.0 M	354.0 G	48.2	69.8	52.8	43.2	67.0	46.1
ViL-S† (Zhang et al, 2021)	45.0 M	218.3 G	47.1	68.7	51.5	42.7	65.9	46.2
ViL-M† (Zhang et al, 2021)	60.1 M	293.8 G	48.9	70.3	54.0	44.2	67.9	47.7
ViL-B† (Zhang et al, 2021)	76.1 M	384.4 G	<b>49.6</b>	70.7	54.6	<b>44.5</b>	68.3	48.0
SG-Former-S (Ren et al, 2023)	41.0 M	-	<b>49.6</b>	71.1	54.5	44.0	68.3	46.9
SG-Former-M (Ren et al, 2023)	51.0 M	-	<b>50.5</b>	71.5	54.9	<b>45.4</b>	68.8	48.2
SG-Former-B (Ren et al, 2023)	95.0 M	-	<b>51.3</b>	72.4	56.0	<b>45.2</b>	69.6	48.8
Mambas								
VMamba-T (Liu et al, 2024g)	50.0 M	270.0 G	<b>48.9</b>	70.6	53.6	<b>43.7</b>	67.7	46.8
VMamba-S (Liu et al, 2024g)	70.0 M	384.0 G	<b>49.9</b>	70.9	54.7	<b>44.2</b>	68.2	47.7
FractalMamba-T (Tang et al, 2024b)	50.0 M	270.0 G	<b>49.5</b>	71.3	54.0	<b>44.1</b>	68.5	47.4
EffVMamba-T (Pei et al, 2024)	11.0 M	60.0 G	38.3	60.3	41.6	35.3	57.2	37.6
EffVMamba-S (Pei et al, 2024)	31.0 M	197.0 G	41.6	63.9	45.6	38.2	60.8	40.7
EffVMamba-B (Pei et al, 2024)	53.0 M	252.0 G	45.0	66.9	49.2	40.8	64.1	43.7
MSVMamba-M (Shi et al, 2024a)	32.0 M	201.0 G	46.3	68.1	50.8	41.8	65.1	44.9
MSVMamba-T (Shi et al, 2024a)	53.0 M	252.0 G	48.3	69.5	53.0	43.2	66.8	46.9
LocalVMamba-T (Huang et al, 2024e)	45.0 M	291.0 G	48.7	70.1	53.0	43.4	67.0	46.4
LocalVMamba-S (Huang et al, 2024e)	69.0 M	414.0 G	<b>49.9</b>	70.5	54.4	<b>44.1</b>	67.8	47.4

## References

- Ali A, Zimmerman I, Wolf L (2024) The hidden attention of mamba models. arXiv preprint arXiv:240301590
- Archit A, Pape C (2024) Vim-unet: Vision mamba for biomedical segmentation. arXiv preprint arXiv:240407705
- Atli OF, Kabas B, Arslan F, Yurt M, Dalmaz O, Çukur T (2024) I2i-mamba: Multi-modal medical image synthesis via selective state space modeling. arXiv preprint arXiv:240514022
- Bai J, Yin Y, He Q (2024) Retinexmamba: Retinex-based mamba for low-light image enhancement. arXiv preprint arXiv:240503349
- Cao Z, Wu X, Deng LJ, Zhong Y (2024) A novel state space model with local enhancement and state sharing for image fusion. arXiv preprint arXiv:240409293
- Caron M, Touvron H, Misra I, Jégou H, Mairal J, Bojanowski P, Joulin A (2021) Emerging properties in self-supervised vision transformers. In: ICCV, pp 9630–9640
- Chaudhuri S, Bhattacharya S (2024) Simba: Mamba augmented u-shiftgcn for skeletal action recognition in videos. arXiv preprint arXiv:240407645
- Chen G, Huang Y, Xu J, Pei B, Chen Z, Li Z, Wang J, Li K, Lu T, Wang L (2024a) Video mamba suite: State space model as a versatile alternative for video understanding. arXiv preprint arXiv:240309626
- Chen H, Hong Y, Huang Z, Xu Z, Gu Z, et al (2024b) Demamba: Ai-generated video detection on million-scale gen-video benchmark. arXiv preprint arXiv:240519707
- Chen H, Song J, Han C, Xia J, Yokoya N (2024c) Changemamba: Remote sensing change detection with spatio-temporal state space model. arXiv preprint arXiv:240403425
- Chen K, Chen B, Liu C, Li W, Zou Z, Shi Z (2024d) Rs-mamba: Remote sensing image classification with state space model. arXiv preprint arXiv:240319654

- Chen T, Tan Z, Gong T, Chu Q, Wu Y, Liu B, Ye J, Yu N (2024e) Mim-istd: Mamba-in-mamba for efficient infrared small target detection. arXiv preprint arXiv:240302148
- Chen Y, Shi H, Liu X, Shi T, Zhang R, Liu D, Xiong Z, Wu F (2024f) Tokenunify: Scalable autoregressive visual pre-training with mixture token prediction. arXiv preprint arXiv:240516847
- Chen Y, Xie J, Lin Y, Song Y, Yang W, Yu R (2024g) Survmamba: State space model with multi-grained multimodal interaction for survival prediction. arXiv preprint arXiv:240408027
- Chen Z, Ge Y (2024) Mambaue: Unraveling the ocean's secrets with only 2.8 flops. arXiv preprint arXiv:240413884
- Chen Z, Duan Y, Wang W, He J, Lu T, Dai J, Qiao Y (2023) Vision transformer adapter for dense predictions. In: ICLR
- Cheng C, Wang H, Sun H (2024) Activating wider areas in image super-resolution. arXiv preprint arXiv:240308330
- Cirone NM, Orvieto A, Walker B, Salvi C, Lyons TJ (2024) Theoretical foundations of deep selective state-space models. arXiv preprint arXiv:240219047
- Dao T, Gu A (2024) Transformers are ssms: Generalized models and efficient algorithms through structured state space duality. arXiv preprint arXiv:240521060
- Darcet T, Oquab M, Mairal J, Bojanowski P (2024) Vision transformers need registers. In: ICLR
- Deng J, Dong W, Socher R, Li L, Li K, Fei-Fei L (2009) Imagenet: A large-scale hierarchical image database. In: CVPR, pp 248–255
- Deng R, Gu T (2024) Cu-mamba: Selective state space models with channel learning for image restoration. arXiv preprint arXiv:240411778
- Devlin J, Chang M, Lee K, Toutanova K (2019) BERT: pre-training of deep bidirectional transformers for language understanding. In: NAACL-HLT, pp 4171–4186
- Dong W, Zhu H, Lin S, Luo X, Shen Y, Liu X, Zhang J, Guo G, Zhang B (2024) Fusion-mamba for cross-modality object detection. arXiv preprint arXiv:240409146
- Dosovitskiy A, Beyer L, Kolesnikov A, Weissenborn D, Zhai X, et al (2021) An image is worth 16x16 words: Transformers for image recognition at scale. In: ICLR
- Du C, Li Y, Xu C (2024) Understanding robustness of visual state space models for image classification. arXiv preprint arXiv:240310935
- Fang Z, Wang Y, Wang Z, Zhang J, Ji X, Zhang Y (2024) Mammil: Multiple instance learning for whole slide images with state space models. arXiv preprint arXiv:240305160
- Fei Z, Fan M, Yu C, Huang J (2024) Scalable diffusion models with state space backbone. arXiv preprint arXiv:240205608
- Friston KJ, Harrison LM, Penny WD (2003) Dynamic causal modelling. *NeuroImage* 19(4):1273–1302
- Fu DY, Dao T, Saab KK, Thomas AW, Rudra A, Ré C (2023) Hungry hungry hippos: Towards language modeling with state space models. In: ICLR
- Fu G, Xiong F, Lu J, Zhou J, Qian Y (2024a) Ssumamba: Spatial-spectral selective state space model for hyperspectral image denoising. arXiv preprint arXiv:240501726
- Fu L, Li X, Cai X, Wang Y, Wang X, Shen Y, Yao Y (2024b) Md-dose: A diffusion model based on the mamba for radiotherapy dose prediction. arXiv preprint arXiv:240308479
- Gao H, Dang D (2024) Learning enriched features via selective state spaces model for efficient image deblurring. arXiv preprint arXiv:240320106
- Gao Y, Huang J, Sun X, Jie Z, Zhong Y, Ma L (2024) Matten: Video generation with mamba-attention. arXiv preprint arXiv:240503025
- Gong H, Kang L, Wang Y, Wan X, Li H (2024) nnmamba: 3d biomedical image segmentation, classification and landmark detection with state space model. arXiv preprint arXiv:240203526
- Grazzi R, Siems J, Schrodi S, Brox T, Hutter F (2024) Is mamba capable of in-context learning? arXiv preprint arXiv:240203170
- Gu A, Dao T (2023) Mamba: Linear-time sequence modeling with selective state spaces. arXiv preprint arXiv:231200752
- Gu A, Dao T, Ermon S, Rudra A, Ré C (2020) Hippo: Recurrent memory with optimal polynomial projections. In: NeurIPS
- Gu A, Johnson I, Goel K, Saab K, Dao T, Rudra A, Ré C (2021) Combining recurrent, convolutional, and continuous-time models with linear state space layers. In: NeurIPS, pp 572–585
- Gu A, Goel K, Gupta A, Ré C (2022a) On the parameterization and initialization of diagonal state space models. In: NeurIPS
- Gu A, Goel K, Ré C (2022b) Efficiently modeling long sequences with structured state spaces. In: ICLR
- Gu A, Johnson I, Timalsina A, Rudra A, Ré C (2023) How to train your HIPPO: state space models with generalized orthogonal basis projections. In: ICLR
- Guan M, Xu H, Jiang G, Yu M, Chen Y, Luo T, Song Y (2024) Watermamba: Visual state space model for underwater image enhancement. arXiv preprint arXiv:240508419
- Guo H, Li J, Dai T, Ouyang Z, Ren X, Xia ST (2024a) Mambair: A simple baseline for image restoration with state-space model. arXiv preprint arXiv:240215648
- Guo T, Wang Y, Shu S, Chen D, Tang Z, Meng C, Bai X (2024b) Mambamorph: a mamba-based framework for medical mr-ct deformable registration. arXiv preprint arXiv:240113934
- Gupta A, Gu A, Berant J (2022) Diagonal state spaces are as effective as structured state spaces. In: NeurIPS
- Hafner D, Lillicrap TP, Ba J, Norouzi M (2020) Dream to control: Learning behaviors by latent imagination. In: ICLR
- Han X, Tang Y, Wang Z, Li X (2024) Mamba3d: Enhancing local features for 3d point cloud analysis via state space model. arXiv preprint arXiv:240414966
- Hao J, He L, Hung KF (2024) T-mamba: Frequency-enhanced gated long-range dependency for tooth 3d cbct segmentation. arXiv preprint arXiv:240401065
- Hasani RM, Lechner M, Wang T, Chahine M, Amini A, Rus D (2023) Liquid structural state-space models. In: ICLR
- He H, Bai Y, Zhang J, He Q, Chen H, Gan Z, Wang C, Li X, Tian G, Xie L (2024a) Mambaad: Exploring state space models for multi-class unsupervised anomaly detection. arXiv preprint arXiv:240406564
- He K, Zhang X, Ren S, Sun J (2016) Deep residual learning for image recognition. In: CVPR, pp 770–778
- He K, Gkioxari G, Dollár P, Girshick RB (2017) Mask R-CNN. In: ICCV, pp 2980–2988
- He X, Cao K, Yan K, Li R, Xie C, Zhang J, Zhou M (2024b) Pan-mamba: Effective pan-sharpening with state space model. arXiv preprint arXiv:240212192
- He Y, Tu B, Liu B, Li J, Plaza A (2024c) 3dss-mamba: 3d-spectral-spatial mamba for hyperspectral image classification. arXiv preprint arXiv:240512487
- Heidari M, Kolahi SG, Karimijafarbigloo S, Azad B, Bozorgpour A, et al (2024) Computation-efficient era: A comprehensive survey of state space models in medical image analysis. arXiv preprint arXiv:240603430
- Hu VT, Baumann SA, Gui M, Grebenkova O, Ma P, Fischer J, Ommer B (2024) Zigma: Zigzag mamba diffusion model.

- arXiv preprint arXiv:240313802
- Huang J, Wang S, Wang S, Wu Z, Wang X, Jiang B (2024a) Mamba-fetrack: Frame-event tracking via state space model. arXiv preprint arXiv:240418174
- Huang J, Yang L, Wang F, Wu Y, Nan Y, Aviles-Rivero AI, Schönlieb CB, Zhang D, Yang G (2024b) Mambamir: An arbitrary-masked mamba for joint medical image reconstruction and uncertainty estimation. arXiv preprint arXiv:240218451
- Huang J, Yang L, Wang F, Wu Y, Nan Y, et al (2024c) Enhancing global sensitivity and uncertainty quantification in medical image reconstruction with monte carlo arbitrary-masked mamba. arXiv preprint arXiv:240517659
- Huang L, Chen Y, He X (2024d) Spectral-spatial mamba for hyperspectral image classification. arXiv preprint arXiv:240418401
- Huang T, Pei X, You S, Wang F, Qian C, Xu C (2024e) Local-mamba: Visual state space model with windowed selective scan. arXiv preprint arXiv:240309338
- Huang W, Shen Y, Yang Y (2024f) Clip-mamba: Clip pre-trained mamba models with ood and hessian evaluation. arXiv preprint arXiv:240419394
- Huang Y, Miyazaki T, Liu X, Omachi S (2024g) Irsr-mamba: Infrared image super-resolution via mamba-based wavelet transform feature modulation model. arXiv preprint arXiv:240509873
- Isensee F, Petersen J, Klein A, Zimmerer D, Jaeger PF, et al (2018) nnu-net: Self-adapting framework for u-net-based medical image segmentation. arXiv preprint arXiv:180910486
- Isensee F, Wald T, Ulrich C, Baumgartner M, Roy S, Maier-Hein K, Jaeger PF (2024) nnu-net revisited: A call for rigorous validation in 3d medical image segmentation. arXiv preprint arXiv:240409556
- Ju Z, Zhou W (2024) Vm-ddpm: Vision mamba diffusion for medical image synthesis. arXiv preprint arXiv:240505667
- Kalman RE (1960) A New Approach to Linear Filtering and Prediction Problems. *Journal of Basic Engineering* 82(1):35–45
- Katharopoulos A, Vyas A, Pappas N, Fleuret F (2020) Transformers are rnns: Fast autoregressive transformers with linear attention. In: *ICML*, vol 119, pp 5156–5165
- Kong L, Dong J, Yang MH, Pan J (2024) Efficient visual state space model for image deblurring. arXiv preprint arXiv:240514343
- Krizhevsky A, Sutskever I, Hinton GE (2012) Imagenet classification with deep convolutional neural networks. In: *NeurIPS*, pp 1106–1114
- Lee BK, Kim CW, Park B, Ro YM (2024) Meteor: Mamba-based traversal of rationale for large language and vision models. arXiv preprint arXiv:240515574
- Lei X, Zhang W, Cao W (2024) Dvmsr: Distillated vision mamba for efficient super-resolution. arXiv preprint arXiv:240503008
- Li D, Liu Y, Fu X, Xu S, Zha ZJ (2024a) Fouriermamba: Fourier learning integration with state space models for image deraining. arXiv preprint arXiv:240519450
- Li H, Hu Q, Yao Y, Yang K, Chen P (2024b) Cfmw: Cross-modality fusion mamba for multispectral object detection under adverse weather conditions. arXiv preprint arXiv:240416302
- Li K, Li X, Wang Y, He Y, Wang Y, Wang L, Qiao Y (2024c) Videomamba: State space model for efficient video understanding. arXiv preprint arXiv:240306977
- Li S, Singh H, Grover A (2024d) Mamba-nd: Selective state space modeling for multi-dimensional data. arXiv preprint arXiv:240205892
- Li W, Hong X, Fan X (2024e) Spikemba: Multi-modal spiking saliency mamba for temporal video grounding. arXiv preprint arXiv:240401174
- Li W, Zhou H, Song Z, Yang W (2024f) Coupled mamba: Enhanced multi-modal fusion with coupled state space model. arXiv preprint arXiv:240518014
- Li Y, Yang W, Fei B (2024g) 3dmambacomplete: Exploring structured state space model for point cloud completion. arXiv preprint arXiv:240407106
- Li Z, Pan H, Zhang K, Wang Y, Yu F (2024h) Mambadfuse: A mamba-based dual-phase model for multi-modality image fusion. arXiv preprint arXiv:240408406
- Li Z, Ren J, Cheng W, Du C, Pan Y, Ling H (2024i) Sparse reconstruction of optical doppler tomography based on state space model. arXiv preprint arXiv:240417484
- Liang D, Zhou X, Wang X, Zhu X, Xu W, Zou Z, Ye X, Bai X (2024) Pointmamba: A simple state space model for point cloud analysis. arXiv preprint arXiv:240210739
- Liao W, Zhu Y, Wang X, Pan C, Wang Y, Ma L (2024) Lightm-unet: Mamba assists in lightweight unet for medical image segmentation. arXiv preprint arXiv:240305246
- Lin T, Maire M, Belongie SJ, Hays J, Perona P, Ramanan D, Dollár P, Zitnick CL (2014) Microsoft COCO: common objects in context. In: *ECCV*, Springer, Lecture Notes in Computer Science, vol 8693, pp 740–755
- Liu C, Chen K, Chen B, Zhang H, Zou Z, Shi Z (2024a) Rscama: Remote sensing image change captioning with state space model. arXiv preprint arXiv:240418895
- Liu J, Han J, Liu L, Aviles-Rivero AI, Jiang C, Liu Z, Wang H (2024b) Mamba4d: Efficient long-sequence point cloud video understanding with disentangled spatial-temporal state space models. arXiv preprint arXiv:240514338
- Liu J, Yang H, Zhou HY, Xi Y, Yu L, et al (2024c) Swin-unamba: Mamba-based unet with imagenet-based pre-training. arXiv preprint arXiv:240203302
- Liu J, Yu R, Wang Y, Zheng Y, Deng T, Ye W, Wang H (2024d) Point mamba: A novel point cloud backbone based on state space model with octree-based ordering strategy. arXiv preprint arXiv:240306467
- Liu M, Dan J, Lu Z, Yu Y, Li Y, Li X (2024e) Cm-unet: Hybrid cnn-mamba unet for remote sensing image semantic segmentation. arXiv preprint arXiv:240510530
- Liu X, Zhang C, Zhang L (2024f) Vision mamba: A comprehensive survey and taxonomy. arXiv preprint arXiv:240504404
- Liu Y, Tian Y, Zhao Y, Yu H, Xie L, Wang Y, Ye Q, Liu Y (2024g) Vmamba: Visual state space model. arXiv preprint arXiv:240110166
- Liu Y, Xiao J, Guo Y, Jiang P, Yang H, Wang F (2024h) Hsmdmamba: Exploring bidirectional state-space models for hyperspectral denoising. arXiv preprint arXiv:240409697
- Liu Z, Lin Y, Cao Y, Hu H, Wei Y, Zhang Z, Lin S, Guo B (2021) Swin transformer: Hierarchical vision transformer using shifted windows. In: *ICCV*, IEEE, pp 9992–10,002
- Liu Z, Hu H, Lin Y, Yao Z, Xie Z, Wei Y, Ning J, Cao Y, Zhang Z, Dong L, Wei F, Guo B (2022a) Swin transformer V2: scaling up capacity and resolution. In: *CVPR*, pp 11,999–12,009
- Liu Z, Mao H, Wu C, Feichtenhofer C, Darrell T, Xie S (2022b) A convnet for the 2020s. In: *CVPR*, pp 11,966–11,976
- Long S, Zhou Q, Li X, Lu X, Ying C, Luo Y, Ma L, Yan S (2024) Dgmamba: Domain generalization via generalized state space model. arXiv preprint arXiv:240407794

- Ma C, Wang Z (2024) Semi-mamba-unet: Pixel-level contrastive and pixel-level cross-supervised visual mamba-based unet for semi-supervised medical image segmentation. arXiv e-prints pp arXiv:2402
- Ma H, Lei S, Celik T, Li HC (2024a) Fer-yolo-mamba: Facial expression detection and classification based on selective state space. arXiv preprint arXiv:240501828
- Ma H, Li H, Cheng C, Wang G, Song X, Wu X (2024b) S4fusion: Saliency-aware selective state space model for infrared visible image fusion. arXiv preprint arXiv:240520881
- Ma HY, Zhang L, Shi S (2024c) Vmambacc: A visual state space model for crowd counting. arXiv preprint arXiv:240503978
- Ma J, Li F, Wang B (2024d) U-mamba: Enhancing long-range dependency for biomedical image segmentation. arXiv preprint arXiv:240104722
- Ma X, Zhang X, Pun MO (2024e) Rs3mamba: Visual state space model for remote sensing images semantic segmentation. arXiv preprint arXiv:240402457
- Meng Z, Yang C, Liu J, Tang H, Zhao P, Wang Y (2024) Instructgie: Towards generalizable image editing. arXiv preprint arXiv:240305018
- Mo S, Tian Y (2024) Scaling diffusion mamba with bidirectional ssms for efficient image and video generation. arXiv preprint arXiv:240515881
- Nasiri-Sarvi A, Trinh VQH, Rivaz H, Hosseini MS (2024) Vim4path: Self-supervised vision mamba for histopathology images. In: Proceedings of the IEEE/CVF Conference on Computer Vision and Pattern Recognition, pp 6894–6903
- Nguyen VT, Pham VT, Tran TT (2024) Ac-mambaseg: An adaptive convolution and mamba-based architecture for enhanced skin lesion segmentation. arXiv preprint arXiv:240503011
- Oppenheim A, Verghese G (2010) Signals, Systems and Inference, Global Edition. Pearson
- Oquab M, Darcet T, Moutakanni T, Vo H, Szafraniec M, et al (2023) Dinov2: Learning robust visual features without supervision. arXiv preprint arXiv:230407193
- Orvieto A, Smith SL, Gu A, Fernando A, Gülçehre Ç, Pascanu R, De S (2023) Resurrecting recurrent neural networks for long sequences. In: ICML, vol 202, pp 26,670–26,698
- Oshima Y, Taniguchi S, Suzuki M, Matsuo Y (2024) Ssm meets video diffusion models: Efficient video generation with structured state spaces. arXiv preprint arXiv:240307711
- Park J, Park J, Xiong Z, Lee N, Cho J, Oymak S, Lee K, Papailiopoulos D (2024) Can mamba learn how to learn? A comparative study on in-context learning tasks. arXiv preprint arXiv:240204248
- Patro BN, Agneeswaran VS (2023) Scattering vision transformer: Spectral mixing matters. In: NeurIPS
- Patro BN, Agneeswaran VS (2024a) Mamba-360: Survey of state space models as transformer alternative for long sequence modelling: Methods, applications, and challenges. arXiv preprint arXiv:240416112
- Patro BN, Agneeswaran VS (2024b) Simba: Simplified mamba-based architecture for vision and multivariate time series. arXiv preprint arXiv:240315360
- Peebles W, Xie S (2023) Scalable diffusion models with transformers. In: ICCV, pp 4172–4182
- Pei X, Huang T, Xu C (2024) Efficientvmamba: Atrous selective scan for light weight visual mamba. arXiv preprint arXiv:240309977
- Peng S, Zhu X, Deng H, Lei Z, Deng LJ (2024) Fusion-mamba: Efficient image fusion with state space model. arXiv preprint arXiv:240407932
- Qian Z, Xiao Z, Wu Z, Yang D, Li M, Wang S, Wang S, Kou D, Zhang L (2024) Smcd: High realism motion style transfer via mamba-based diffusion. arXiv preprint arXiv:240502844
- Qiao Y, Yu Z, Guo L, Chen S, Zhao Z, Sun M, Wu Q, Liu J (2024) V1-mamba: Exploring state space models for multi-modal learning. arXiv preprint arXiv:240313600
- Qin S, Wang J, Zhou Y, Chen B, Luo T, An B, Dai T, Xia S, Wang Y (2024) Mambavc: Learned visual compression with selective state spaces. arXiv preprint arXiv:240515413
- Radosavovic I, Kosaraju RP, Girshick RB, He K, Dollár P (2020) Designing network design spaces. In: CVPR, pp 10,425–10,433
- Ren H, Zhou Y, Zhu J, Fu H, Huang Y, Lin X, Fang Y, Ma F, Yu H, Cheng B (2024a) Rethinking efficient and effective point-based networks for event camera classification and regression: Eventmamba. arXiv preprint arXiv:240506116
- Ren S, Yang X, Liu S, Wang X (2023) Sg-former: Self-guided transformer with evolving token reallocation. In: ICCV, pp 5980–5991
- Ren S, Li X, Tu H, Wang F, Shu F, Zhang L, Mei J, Yang L, Wang P, Wang H, Yuille A, Xie C (2024b) Autoregressive pretraining with mamba in vision. arXiv preprint arXiv:240607537
- Rombach R, Blattmann A, Lorenz D, Esser P, Ommer B (2022) High-resolution image synthesis with latent diffusion models. In: CVPR, pp 10,674–10,685
- Ruan J, Xiang S (2024) Vm-unet: Vision mamba unet for medical image segmentation. arXiv preprint arXiv:240202491
- Sandler M, Howard AG, Zhu M, Zhmoginov A, Chen L (2018) Mobilenetv2: Inverted residuals and linear bottlenecks. In: CVPR, pp 4510–4520
- Sanjid KS, Hossain MT, Junayed MSS, Uddin DMM (2024a) Integrating mamba sequence model and hierarchical up-sampling network for accurate semantic segmentation of multiple sclerosis legion. arXiv preprint arXiv:240317432
- Sanjid KS, Hossain MT, Junayed MSS, Uddin MM (2024b) Optimizing universal lesion segmentation: State space model-guided hierarchical networks with feature importance adjustment. arXiv preprint arXiv:240417235
- Shao Z, Bian H, Chen Y, Wang Y, Zhang J, et al (2021) Transmil: Transformer based correlated multiple instance learning for whole slide image classification. Advances in neural information processing systems 34:2136–2147
- Sharma AS, Atkinson D, Bau D (2024) Locating and editing factual associations in mamba. arXiv preprint arXiv:240403646
- Shen Q, Yi X, Wu Z, Zhou P, Zhang H, Yan S, Wang X (2024) Gamba: Marry gaussian splatting with mamba for single view 3d reconstruction. arXiv preprint arXiv:240318795
- Shi F, Chen X, Misra K, Scales N, Dohan D, Chi EH, Schärli N, Zhou D (2023) Large language models can be easily distracted by irrelevant context. In: ICML, vol 202, pp 31,210–31,227
- Shi Y, Dong M, Xu C (2024a) Multi-scale vmamba: Hierarchy in hierarchy visual state space model. arXiv preprint arXiv:240514174
- Shi Y, Xia B, Jin X, Wang X, Zhao T, Xia X, Xiao X, Yang W (2024b) Vmambair: Visual state space model for image restoration. arXiv preprint arXiv:240311423
- Shou Y, Meng T, Zhang F, Yin N, Li K (2024) Revisiting multi-modal emotion learning with broad state space



- models and probability-guidance fusion. arXiv preprint arXiv:240417858
- Simonyan K, Zisserman A (2015) Very deep convolutional networks for large-scale image recognition. In: ICLR
- Smith JTH, Warrington A, Linderman SW (2023) Simplified state space layers for sequence modeling. In: ICLR
- Tang H, Cheng L, Huang G, Tan Z, Lu J, Wu K (2024a) Rotate to scan: Unet-like mamba with triplet ssm module for medical image segmentation. arXiv preprint arXiv:240317701
- Tang L, Xiao H, Jiang PT, Zhang H, Chen J, Li B (2024b) Scalable visual state space model with fractal scanning. arXiv preprint arXiv:240514480
- Teng Y, Wu Y, Shi H, Ning X, Dai G, Wang Y, Li Z, Liu X (2024) Dim: Diffusion mamba for efficient high-resolution image synthesis. arXiv preprint arXiv:240514224
- Touvron H, Cord M, Douze M, Massa F, Sablayrolles A, Jégou H (2021) Training data-efficient image transformers & distillation through attention. In: ICML, vol 139, pp 10,347–10,357
- Touvron H, Cord M, Jégou H (2022) Deit III: revenge of the vit. In: ECCV, Springer, vol 13684, pp 516–533
- Touvron H, Lavril T, Izacard G, Martinet X, Lachaux MA, et al (2023) Llama: Open and efficient foundation language models. arXiv preprint arXiv:230213971
- Tsai TY, Lin L, Hu S, Zhu H, Wang X, et al (2024) Uu-mamba: Uncertainty-aware u-mamba for cardiac image segmentation. arXiv preprint arXiv:240517496
- Tustin A (1947) A method of analysing the behaviour of linear systems in terms of time series. *Journal of the Institution of Electrical Engineers-Part IIA: Automatic Regulators and Servo Mechanisms* 94(1):130–142
- Vaswani A, Shazeer N, Parmar N, Uszkoreit J, Jones L, Gomez AN, Kaiser L, Polosukhin I (2017) Attention is all you need. In: NeurIPS, pp 5998–6008
- Verma T, Singh J, Bhartari Y, Jarwal R, Singh S, Singh S (2024) Soar: Advancements in small body object detection for aerial imagery using state space models and programmable gradients. arXiv preprint arXiv:240501699
- Wan Z, Wang Y, Yong S, Zhang P, Stepputtis S, Sycara K, Xie Y (2024) Sigma: Siamese mamba network for multi-modal semantic segmentation. arXiv preprint arXiv:240404256
- Wang F, Wang J, Ren S, Wei G, Mei J, Shao W, Zhou Y, Yuille A, Xie C (2024a) Mamba-r: Vision mamba also needs registers. arXiv preprint arXiv:240514858
- Wang G, Zhang X, Peng Z, Zhang T, Jia X, Jiao L (2024b) S2mamba: A spatial-spectral state space model for hyperspectral image classification. arXiv preprint arXiv:240418213
- Wang J, Chen J, Chen D, Wu J (2024c) Large window-based mamba unet for medical image segmentation: Beyond convolution and self-attention. arXiv preprint arXiv:240307332
- Wang P, Wang X, Luo H, Zhou J, Zhou Z, Wang F, Li H, Jin R (2022a) Scaled relu matters for training vision transformers. In: AAAI, pp 2495–2503
- Wang Q, Wang C, Lai Z, Zhou Y (2024d) Insectmamba: Insect pest classification with state space model. arXiv preprint arXiv:240403611
- Wang S, Li Q (2024) Stablessm: Alleviating the curse of memory in state-space models through stable reparameterization. ICML
- Wang W, Xie E, Li X, Fan D, Song K, Liang D, Lu T, Luo P, Shao L (2022b) PVT v2: Improved baselines with pyramid vision transformer. *Comput Vis Media* 8(3):415–424
- Wang X, Huang Z, Zhang S, Zhu J, Feng L (2024e) Gmsr:gradient-guided mamba for spectral reconstruction from rgb images. arXiv preprint arXiv:240507777
- Wang X, Kang Z, Mu Y (2024f) Text-controlled motion mamba: Text-instructed temporal grounding of human motion. arXiv preprint arXiv:240411375
- Wang X, Wang S, Ding Y, Li Y, Wu W, Rong Y, Kong W, Huang J, Li S, Yang H, Wang Z, Jiang B, Li C, Wang Y, Tian Y, Tang J (2024g) State space model for new-generation network alternative to transformers: A survey. arXiv preprint arXiv:240409516
- Wang Z, Ma C (2024) Weak-mamba-unet: Visual mamba makes cnn and vit work better for scribble-based medical image segmentation. arXiv preprint arXiv:240210887
- Wang Z, Chen Z, Wu Y, Zhao Z, Zhou L, Xu D (2024h) Pointramamba: A hybrid transformer-mamba framework for point cloud analysis. arXiv preprint arXiv:240515463
- Wang Z, Zheng JQ, Ma C, Guo T (2024i) Vmambamorph: a multi-modality deformable image registration framework based on visual state space model with cross-scan module. arXiv preprint arXiv:240405105
- Wang Z, Zheng JQ, Zhang Y, Cui G, Li L (2024j) Mamba-unet: Unet-like pure visual mamba for medical image segmentation. arXiv preprint arXiv:240205079
- Wu R, Liu Y, Liang P, Chang Q (2024a) H-vmunet: High-order vision mamba unet for medical image segmentation. arXiv preprint arXiv:240313642
- Wu R, Liu Y, Liang P, Chang Q (2024b) Ultralight vm-unet: Parallel vision mamba significantly reduces parameters for skin lesion segmentation. arXiv preprint arXiv:240320035
- Xiang Q, Cheng J, Luo J, Wu J, Fan R, Chen X, Tang X (2024) Overlapmamba: Novel shift state space model for lidar-based place recognition. arXiv preprint arXiv:240507966
- Xiao T, Liu Y, Zhou B, Jiang Y, Sun J (2018) Unified perceptual parsing for scene understanding. In: ECCV, Springer, vol 11209, pp 432–448
- Xiao Y, Yuan Q, Jiang K, Chen Y, Zhang Q, Lin CW (2024) Frequency-assisted mamba for remote sensing image super-resolution. arXiv preprint arXiv:240504964
- Xie J, Liao R, Zhang Z, Yi S, Zhu Y, Luo G (2024a) Promamba: Prompt-mamba for polyp segmentation. arXiv preprint arXiv:240313660
- Xie X, Cui Y, leong CI, Tan T, Zhang X, Zheng X, Yu Z (2024b) Fusionmamba: Dynamic feature enhancement for multimodal image fusion with mamba. arXiv preprint arXiv:240409498
- Xing Z, Ye T, Yang Y, Liu G, Zhu L (2024) Segmamba: Long-range sequential modeling mamba for 3d medical image segmentation. arXiv preprint arXiv:240113560
- Xu J (2024) Hc-mamba: Vision mamba with hybrid convolutional techniques for medical image segmentation. arXiv preprint arXiv:240505007
- Yamashita S, Ikehara M (2024) Image deraining with frequency-enhanced state space model. arXiv preprint arXiv:240516470
- Yang C, Chen Z, Espinosa M, Ericsson L, Wang Z, Liu J, Crowley EJ (2024a) Plainmamba: Improving non-hierarchical mamba in visual recognition. arXiv preprint arXiv:240317695
- Yang G, Du K, Yang Z, Du Y, Zheng Y, Wang S (2024b) Cmvim: Contrastive masked vim autoencoder for 3d multi-modal representation learning for ad classification. arXiv preprint arXiv:240316520
- Yang S, Wang Y, Chen H (2024c) Mambamil: Enhancing long sequence modeling with sequence reordering in computa-

- tional pathology. arXiv preprint arXiv:240306800
- Yang Y, Ma C, Yao J, Zhong Z, Zhang Y, Wang Y (2024d) Remamber: Referring image segmentation with mamba twister. arXiv preprint arXiv:240317839
- Yang Y, Xing Z, Huang C, Zhu L (2024e) Vivim: a video vision mamba for medical video object segmentation. arXiv preprint arXiv:240114168
- Yang Z, Zhang J, Wang G, Kalra MK, Yan P (2024f) Cardiovascular disease detection from multi-view chest x-rays with bi-mamba. arXiv preprint arXiv:240518533
- Yao J, Hong D, Li C, Chanussot J (2024) Spectralmamba: Efficient mamba for hyperspectral image classification. arXiv preprint arXiv:240408489
- Yao T, Pan Y, Li Y, Ngo C, Mei T (2022) Wave-vit: Unifying wavelet and transformers for visual representation learning. In: ECCV, vol 13685, pp 328–345
- Ye Z, Chen T (2024) P-mamba: Marrying perona malik diffusion with mamba for efficient pediatric echocardiographic left ventricular segmentation. arXiv preprint arXiv:240208506
- Yu W, Wang X (2024) Mambabout: Do we really need mamba for vision? arXiv preprint arXiv:240507992
- Yuan C, Zhao D, Agaian SS (2024) Mucm-net: A mamba powered ucm-net for skin lesion segmentation. arXiv preprint arXiv:240515925
- Yuan L, Hou Q, Jiang Z, Feng J, Yan S (2023) VOLO: vision outlooker for visual recognition. IEEE Trans Pattern Anal Mach Intell 45(5):6575–6586
- Yue Y, Li Z (2024) Medmamba: Vision mamba for medical image classification. arXiv preprint arXiv:240303849
- Zha Y, Li N, Wang Y, Dai T, Guo H, Chen B, Wang Z, Ouyang Z, Xia ST (2024) Lcm: Locally constrained compact point cloud model for masked point modeling. arXiv preprint arXiv:240517149
- Zhai X, Mustafa B, Kolesnikov A, Beyer L (2023) Sigmoid loss for language image pre-training. In: Proceedings of the IEEE/CVF International Conference on Computer Vision, pp 11,975–11,986
- Zhang H, Zhu Y, Wang D, Zhang L, Chen T, Ye Z (2024a) A survey on visual mamba. arXiv preprint arXiv:240415956
- Zhang J, Bian K, Cheng P, An W, Liu J, Zhou J (2024b) Vim-f: Visual state space model benefiting from learning in the frequency domain. arXiv preprint arXiv:240518679
- Zhang M, Yu Y, Gu L, Lin T, Tao X (2024c) Vm-unet-v2 rethinking vision mamba unet for medical image segmentation. arXiv preprint arXiv:240309157
- Zhang P, Dai X, Yang J, Xiao B, Yuan L, Zhang L, Gao J (2021) Multi-scale vision longformer: A new vision transformer for high-resolution image encoding. In: iccv21/vil, pp 2978–2988
- Zhang T, Li X, Yuan H, Ji S, Yan S (2024d) Point could mamba: Point cloud learning via state space model. arXiv preprint arXiv:240300762
- Zhang Z, Liu A, Reid I, Hartley R, Zhuang B, Tang H (2024e) Motion mamba: Efficient and long sequence motion generation with hierarchical and bidirectional selective ssm. arXiv preprint arXiv:240307487
- Zhao H, Zhang M, Zhao W, Ding P, Huang S, Wang D (2024a) Cobra: Extending mamba to multi-modal large language model for efficient inference. arXiv preprint arXiv:240314520
- Zhao S, Chen H, Zhang X, Xiao P, Bai L, Ouyang W (2024b) Rs-mamba for large remote sensing image dense prediction. arXiv preprint arXiv:240402668
- Zhen Z, Hu Y, Feng Z (2024) Freqmamba: Viewing mamba from a frequency perspective for image deraining. arXiv preprint arXiv:240409476
- Zheng Z, Wu C (2024) U-shaped vision mamba for single image dehazing. arXiv preprint arXiv:240204139
- Zheng Z, Zhang J (2024) Fd-vision mamba for endoscopic exposure correction. arXiv preprint arXiv:240206378
- Zhou B, Zhao H, Puig X, Xiao T, Fidler S, Barriuso A, Torralba A (2019) Semantic understanding of scenes through the ADE20K dataset. Int J Comput Vis 127(3):302–321
- Zhou H, Wu X, Chen H, Chen X, He X (2024a) Rsdehamba: Lightweight vision mamba for remote sensing satellite image dehazing. arXiv preprint arXiv:240510030
- Zhou Q, Yang W, Fei B, Xu J, Zhang R, Liu K, Luo Y, He Y (2024b) 3dmambaipf: A state space model for iterative point cloud filtering via differentiable rendering. arXiv preprint arXiv:240405522
- Zhou W, Kamata SI, Wang H, Wong MS, et al (2024c) Mamba-in-mamba: Centralized mamba-cross-scan in tokenized mamba model for hyperspectral image classification. arXiv preprint arXiv:240512003
- Zhu L, Liao B, Zhang Q, Wang X, Liu W, Wang X (2024a) Vision mamba: Efficient visual representation learning with bidirectional state space model. arXiv preprint arXiv:240109417
- Zhu Q, Cai Y, Fang Y, Yang Y, Chen C, Fan L, Nguyen A (2024b) Samba: Semantic segmentation of remotely sensed images with state space model. arXiv preprint arXiv:240401705
- Zhu Q, Fang Y, Cai Y, Chen C, Fan L (2024c) Rethinking scanning strategies with vision mamba in semantic segmentation of remote sensing imagery: An experimental study. arXiv preprint arXiv:240508493
- Zou B, Guo Z, Hu X, Ma H (2024a) Rhythmmamba: Fast remote physiological measurement with arbitrary length videos. arXiv preprint arXiv:240406483
- Zou Y, Chen Y, Li Z, Zhang L, Zhao H (2024b) Venturing into uncharted waters: The navigation compass from transformer to mamba. arXiv preprint arXiv:240616722